



HAL
open science

Polycomb Repressive Complex 2 Controls the Embryo-to-Seedling Phase Transition

Daniel Bouyer, François Roudier, Maren Heese, Ellen D. Andersen, Delphine Gey, Moritz K. Nowack, Justin Goodrich, Jean-Pierre J.-P. Renou, Paul E. Grini, Vincent Colot, et al.

► **To cite this version:**

Daniel Bouyer, François Roudier, Maren Heese, Ellen D. Andersen, Delphine Gey, et al.. Polycomb Repressive Complex 2 Controls the Embryo-to-Seedling Phase Transition. PLoS Genetics, 2011, 7 (3), pp.e1002014. 10.1371/journal.pgen.1002014 . hal-02647278

HAL Id: hal-02647278

<https://hal.inrae.fr/hal-02647278>

Submitted on 29 May 2020

HAL is a multi-disciplinary open access archive for the deposit and dissemination of scientific research documents, whether they are published or not. The documents may come from teaching and research institutions in France or abroad, or from public or private research centers.

L'archive ouverte pluridisciplinaire **HAL**, est destinée au dépôt et à la diffusion de documents scientifiques de niveau recherche, publiés ou non, émanant des établissements d'enseignement et de recherche français ou étrangers, des laboratoires publics ou privés.

Polycomb Repressive Complex 2 Controls the Embryo-to-Seedling Phase Transition

Daniel Bouyer¹, Francois Roudier², Maren Heese¹, Ellen D. Andersen³, Delphine Gey⁴, Moritz K. Nowack^{5,6}, Justin Goodrich⁷, Jean-Pierre Renou⁴, Paul E. Grini³, Vincent Colot², Arp Schnittger^{1*}

1 Department of Molecular Mechanisms of Phenotypic Plasticity, Institut de Biologie Moléculaire des Plantes du CNRS, Université de Strasbourg, Strasbourg, France, **2** Institut de Biologie de l'École Normale Supérieure, CNRS UMR 8197–INSERM U 1024, Paris, France, **3** Department of Molecular Biosciences, University of Oslo, Oslo, Norway, **4** Department of Plant Genomics Research, CNRS/INRA, Evry, France, **5** Department of Plant Systems Biology, VIB, Gent, Belgium, **6** Department of Plant Biotechnology and Genetics, Ghent University, Ghent, Belgium, **7** Institute of Molecular Plant Science, University of Edinburgh, Edinburgh, United Kingdom

Abstract

Polycomb repressive complex 2 (PRC2) is a key regulator of epigenetic states catalyzing histone H3 lysine 27 trimethylation (H3K27me3), a repressive chromatin mark. PRC2 composition is conserved from humans to plants, but the function of PRC2 during the early stage of plant life is unclear beyond the fact that it is required for the development of endosperm, a nutritive tissue that supports embryo growth. Circumventing the requirement of PRC2 in endosperm allowed us to generate viable homozygous null mutants for *FERTILIZATION INDEPENDENT ENDOSPERM* (*FIE*), which is the single *Arabidopsis* homolog of Extra Sex Combs, an indispensable component of *Drosophila* and mammalian PRC2. Here we show that H3K27me3 deposition is abolished genome-wide in *fie* mutants demonstrating the essential function of PRC2 in placing this mark in plants as in animals. In contrast to animals, we find that PRC2 function is not required for initial body plan formation in *Arabidopsis*. Rather, our results show that *fie* mutant seeds exhibit enhanced dormancy and germination defects, indicating a deficiency in terminating the embryonic phase. After germination, *fie* mutant seedlings switch to generative development that is not sustained, giving rise to neoplastic, callus-like structures. Further genome-wide studies showed that only a fraction of PRC2 targets are transcriptionally activated in *fie* seedlings and that this activation is accompanied in only a few cases with deposition of H3K4me3, a mark associated with gene activity and considered to act antagonistically to H3K27me3. Up-regulated PRC2 target genes were found to act at different hierarchical levels from transcriptional master regulators to a wide range of downstream targets. Collectively, our findings demonstrate that PRC2-mediated regulation represents a robust system controlling developmental phase transitions, not only from vegetative phase to flowering but also especially from embryonic phase to the seedling stage.

Citation: Bouyer D, Roudier F, Heese M, Andersen ED, Gey D, et al. (2011) Polycomb Repressive Complex 2 Controls the Embryo-to-Seedling Phase Transition. *PLoS Genet* 7(3): e1002014. doi:10.1371/journal.pgen.1002014

Editor: Gregory P. Copenhaver, The University of North Carolina at Chapel Hill, United States of America

Received: November 2, 2010; **Accepted:** January 11, 2011; **Published:** March 10, 2011

Copyright: © 2011 Bouyer et al. This is an open-access article distributed under the terms of the Creative Commons Attribution License, which permits unrestricted use, distribution, and reproduction in any medium, provided the original author and source are credited.

Funding: The work in the laboratory of VC is supported by grants from the French Agence Nationale de la Recherche (ANR Genoplante projects TAG and REGENEOME), in the team of PEG by a FUGE Young Investigator Starting Grant from the Norwegian Research Council (Grant # 510/183190), and in the laboratory of JG by grant F00742 from the UK BBSRC Research council. This work was supported by an ERA-PG grant to PEG and AS, an ATIP grant from the CNRS to AS, and an ERC starting grant from the European Union to AS. The funders had no role in study design, data collection and analysis, decision to publish, or preparation of the manuscript.

Competing Interests: The authors have declared that no competing interests exist.

* E-mail: Arp.Schnittger@ibmp-cnrs.unistra.fr

Introduction

One common principle of flowering plants and probably one of the main reasons for their evolutionary success is the alternation of a dormant seed stage with a growing plant that will eventually reproduce and again generate seeds. Seeds harbor not only the plant embryo, i.e. the next plant generation, but typically contain a nourishing tissue, called the endosperm that supports embryo growth and often provides the nutrients for the germinating seedling. Moreover, the embryo and the endosperm are protected by a hard shell, the seed coat, that also facilitates the distribution of seeds. Remarkably, seeds often will stay dormant after ripening and require for germination a defined order of environmental conditions reflecting the progression of the seasons in moderate climates, i.e. they will germinate only after exposure to warmth after a period of cold temperatures. Many factors have been identified to influence this transition from a dormant embryonic

phase to a germinating seedling (for review see [1]). However, a unifying molecular framework has not been established so far.

For the other major phase transition in plants, e.g. from vegetative growth to flowering, it has been found that Polycomb repressive complex 2 (PRC2) regulation is crucial [2–4]. PRC2 activity was also found to be required for repression of flower formation in young seedlings indicating a function in maintaining and/or establishing vegetative growth [5,6]. Moreover, severely compromising PRC2 function revealed its function in maintaining overall cell and tissue organization, e.g. the distinction between root and shoot fates [5,6].

PRC2 catalyzes the deposition of trimethylation of Lysine 27 on histone H3 (H3K27me3), a repressive chromatin mark [7,8]. The core PRC2 complex is conserved between animals and plants and contains at least four components, which were first identified in *Drosophila*: the HMTase Enhancer of Zeste (E(Z)), the WD40 domain protein Extra sex combs (ESC), the Zn-finger protein

Author Summary

Epigenetic regulation of gene expression through modifications of histone tails is fundamental for growth and development of multicellular organisms. The trimethylation of lysine 27 of histone 3 (H3K27me3) is the landmark of Polycomb Repressive Complex2 (PRC2) function and is associated with gene repression. Here we present the development of a genetic system to generate homozygous null mutants of Arabidopsis PRC2. A first major finding is that H3K27me3 is globally lost in these mutants. Surprisingly, we found that initial body plan organization and embryo development is largely independent of PRC2 action, which is in sharp contrast to embryonic lethality of PRC2 mutants in animals. However, we show here that PRC2 is required to switch from embryonic to seedling phase, and mutant seeds showed enhanced dormancy and germination defects. Indeed, many genes controlling seed maturation and dormancy are marked by H3K27me3 and are upregulated upon loss of PRC2. The invention of seed dormancy of land plants is regarded as one of the major reasons for the evolutionary success of flowering plants, and the here-discovered key role of PRC2 during the developmental phase transition from embryo to seedling growth reveals the adaptation of conserved molecular mechanisms to carry out new functions.

Suppressor of zeste-12 (SU(Z)12) and the nucleosome-remodeling factor 55 (NURF-55) [9–12]. *Arabidopsis* contains three presumptive H3K27me3 HMTases, CURLY LEAF (CLF), SWINGER (SWN) and MEDEA (MEA) that have been found to at least partially compensate for each other. Similarly, *Drosophila* Su(Z)12 function is represented by three partially redundantly acting genes, EMBRYONIC FLOWER 2 (EMF2), FERTILIZATION INDEPENDENT SEED DEVELOPMENT 2 (FIS2), and VERNALIZATION 2 (VRN2). The homolog of *Drosophila* ESC, FIE, is the only PRC2 component that is represented by a single member in *Arabidopsis*.

In the past few years, much progress has been made in the understanding of the *modus operandi* of PRC2. However, a major obstacle in studying the function of chromatin regulators is their essential role in early development as for instance mutants in ESC in *Drosophila* and its murine ortholog EED are embryonic lethal [13–15]. Similarly, PRC2 function is crucial already for endosperm formation in flowering plants by controlling the parent-of-origin dependent activity of a number of genes in the endosperm (imprinting). PRC2 function is maternal gametophytically required and loss of the maternal PRC2 function releases targets genes from their repression leading to endosperm overproliferation and ultimately to seed abortion [16–19]. This requirement for endosperm formation has also precluded so far an analysis of PRC2 action during later stages of seed development and it also remained an open question whether PRC2 function is required for initial body plan formation in flowering plants during which an embryo with shoot, root, and one (Monocotyledons) or two (Dicotyledons) cotyledons is formed. In contrast to animals, the two stem cell populations established in embryogenesis, i.e. the root and shoot meristem, will produce the body of the adult plant and it has been shown previously that PRC2 is involved in postembryonic shoot meristem function [20].

We and others have previously identified a mutant in the cell cycle regulator *CDKA;1* in which the second mitosis during pollen development is missing or substantially delayed [21–23]. However, mutant pollen can successfully fertilize the egg cell giving rise to an embryo while triggering the onset of endosperm development without a paternal contribution. This type of fertilization was

found to bypass the maternal requirement of PRC2-dependent repression during endosperm development resulting in a mutual rescue of the paternal effect of *cdka;1* mutant pollen and the maternal effect caused by mutations in *MEA*, *FIS2* or *FIE* [24].

Here we have used *cdka;1* mutant fertilization to generate homozygous *fie* mutant plants allowing us to functionally address the requirement of PRC2 action during embryogenesis and subsequent plant growth and development. Our results show that PRC2 is required neither for the generation nor maintenance of embryonic organization in striking contrast to animal PRC2 function. However, PRC2 in plants is vital for the reprogramming of developmental fates mediating the switch from embryonic states to growing seedlings. Furthermore, our genome-wide ChIP- and transcriptional profiling experiments gave insights into the circuitry of PRC2 action indicating that developmental phase transitions are robustly controlled by PRC2 through simultaneously targeting genes at different hierarchical levels and triggering positive feed back loops. This network design allows the transduction of environmental cues into stable and self-maintaining developmental fates likely underlying the enormously adaptable yet enduring growth of plants.

Results

Generation of homozygous *fie* mutant plants

Since the female gametophytic defect of mutants in *FIS* class genes can be bypassed by fertilization with *cdka;1* mutant pollen [24], we asked whether this would allow the generation of homozygous *fie* mutant plants in crosses of heterozygous *fie* mutant mother plants with pollen of *cdka;1-fie* double heterozygous plants. Indeed, in the progeny of this cross and amid the descendents of a self-pollinated double heterozygous *cdka;1-fie* mutant a morphologically distinguishable class of plants was identified that was never found among the progeny of heterozygous *fie* or *cdka;1* mutants. Subsequent genotyping confirmed that these plants were homozygous mutant for *fie* (Figure 1). Reciprocal crosses corroborated that the appearance of *fie* resulted solely from fertilization with paternal *cdka;1* whereas maternal *cdka;1* did not contribute to the generation of viable *fie* mutants (Table 1).

The *fie* mutant used as reference allele in this study is a T-DNA insertion line in a central exon and represents a transcriptional null mutant (Figure S1). In the same way generated homozygous seedlings for three additional *fie* alleles resulted in the same mutant phenotype (Figure S1 and data not shown). Thus, circumventing the requirement of FIS action in the endosperm is sufficient to generate homozygous null mutants for the PRC2 core gene *FIE*.

Homozygous *fie* mutants display a progressive mutant phenotype

Loss of ESC function in flies or mammals causes embryo lethality and is essential for the patterning of the body plan [15,25]. In contrast, macro- and microscopical analyses revealed that *fie* mutant seedlings initially showed a wild-type-like body plan with a root and a shoot, two cotyledons, and newly forming rosette leaves that were at this stage morphologically indistinguishable from wild-type sister plants (Figure 1A, 1D). However, *fie* mutants grew more slowly than the wild type and around 10 days after stratification (10 DAS) already initiated flower buds (Figure 1E shows a flower bud at 15 DAS) whereas the wild type started to flower only after more than 30 DAS. During the next 10 days, homozygous *fie* mutants developed an increasing number of ectopic cells (Figure 1K, 1L) and organs (Figure 1H, 1I), showed signs of organ transformations (Figure 1G) and generated somatic embryos (Figure 1J). The loss of spatial and temporal organization

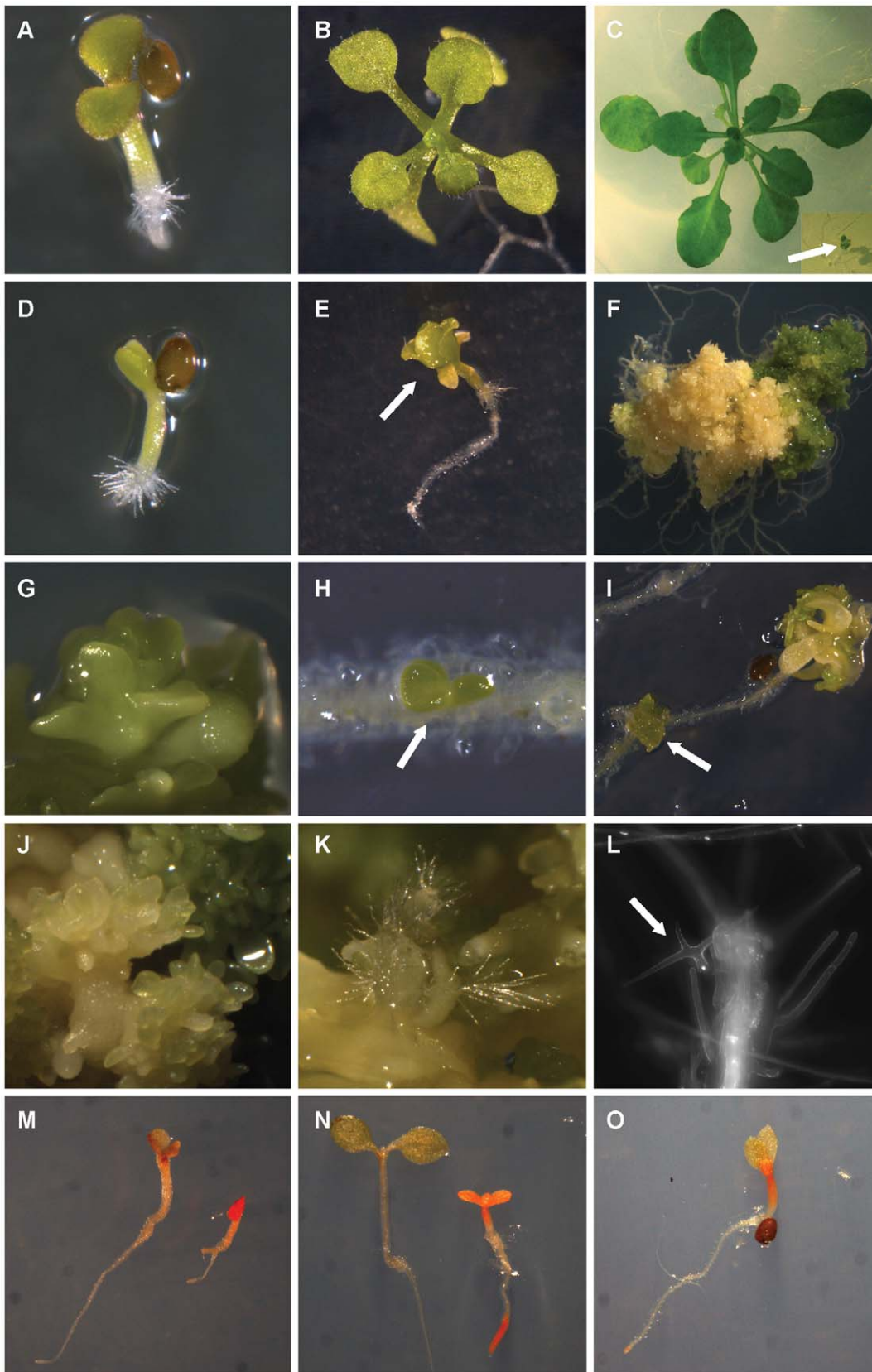


Figure 1. Phenotypic analysis of postembryonic development. Comparison between wild type (A–C) and *fie* mutant (C–L) development. (A) Wild type seedling at 5 DAS. (D) *fie* mutants resemble wild type plants at 5 DAS besides a reduction in growth. (B) Wild-type seedlings are in a vegetative phase at 15 DAS and under day-neutral growth conditions will start to bolt when one month old in contrast to (E) *fie* mutants that show flowers (arrow) already at 15 DAS. (C) Vegetative growth leads to major increase in size of a wild-type plant (left) after 40 DAS whereas a *fie* mutant

plant (right) of the same age is much smaller (arrow). (F) 3 month-old *fie* mutant that has transformed into a callus-like structure. Examples of transformed and/or misplaced organs and cells in *fie* mutants (G–L). (G) Flower-like organs. (H) Leaves (arrow) develop from roots, which are able to transform into offshoots (l, arrow). (J) Somatic embryos are formed in high frequency. (K) Root hairs form at shoot tissue. (L) Leaf hairs (arrow) grow out from roots. Sugar-dependent lipid accumulation in WT and *fie* (M–O). Wild-type and *fie* mutant seedlings were stained with fat-red to visualize lipid accumulation at 5 DAS (M) or at 8 DAS (N). Whereas at early stages there is still a clear staining visible in wild type (M, left side), there is only a faint red signal detectable at 8 DAS (N, left). In contrast, *fie* shows strong staining in cotyledons and roots at both time points (M,N, right side). The lipid accumulation in *fie* is dependent on sugar, as mutants germinating on sugar-free medium show a strong reduction in staining (O). doi:10.1371/journal.pgen.1002014.g001

continued and homozygous *fie* seedlings transformed into callus-like structures that could be maintained for several months displaying an increasing number of small cells (Figure 1F). This neoplastic behavior was confirmed by flow cytometrical analyses showing that shortly after germination *fie* cells started to endo-replicate as a sign of differentiation, a cellular behavior typically found in maturing wild-type plants (Figure S2A, S2B, S2D) [26], whereas at three months after germination the peaks corresponding to 8C and 16C were very much reduced and the remaining cell population gave rise to a DNA profile with cells being mostly in a G1 and a G2 phase, suggesting a massively dividing cell population (Figure S2C, S2D).

Thus, PRC2 in plants does not appear to be required for initial body plan organization, indicating a major difference with animal PRC2 function. After germination homozygous *fie* mutants displayed a progressive loss of cell differentiation states resembling the previously characterized *clf-swn* double mutant or a special *fie* mutant allele that results from the incomplete rescue of a *fie* mutant with a *FIE*-expressing transgene [5,6].

H3K27me3 is lost in homozygous *fie* mutants

As H3K27me3 is essential in animal embryogenesis we asked if this mark is in fact missing in the viable *fie* mutants. Therefore we first analyzed by immuno-cytology the distribution of H3K27me3

in the nuclei of wild-type control plants and homozygous *fie* mutants (Figure S3). In two-week old wild-type plants, a clear nuclear signal that is widely dispersed along the entire chromatin was found (Figure S3A–S3C) consistent with previous studies [27,28]. The spotted antibody signal is excluded from compacted heterochromatic regions, as visualized by DAPI staining. In contrast, no signal was observed in nuclei of two-week old *fie* plants (Figure S3D–S3F).

To obtain a high-resolution molecular map of the genome-wide distribution of H3K27me3 in wild type versus *fie* seedlings, chromatin immunoprecipitation (ChIP) was performed, followed by hybridization to a whole genome tiling array. A total of 5634 genes were identified as putative PRC2 targets in wild type seedlings, in good agreement (68% overlap) with a previous analysis (Table S1, Figure S4) [29].

In *fie* seedlings, the H3K27me3 signal was absent or extremely reduced throughout the genome (Figure 2). However, out of 5634 H3K27me3 positive genes in wild type, 1384 (24.6%) still passed the detection threshold in *fie* seedlings (Figure S4). Furthermore, 2014 genes appeared to be marked *de novo* by H3K27me3 in *fie*. Yet, in addition to being much weaker, the H3K27me3 signal in *fie* showed an atypical distribution pattern over genes and the marked genes were on average larger and slightly closer to transposable elements (Figure S5, Table S2). Notably, the most prominent signal in the mutant was found over heterochromatic regions, i.e. repeat-regions and transposable elements although H3K27me3 is typically excluded from these locations (Figure 2A, Figure S5B) [29]. Such an apparent re-localization of H3K27me3 signal to heterochromatic regions has also been seen on immuno-localization level in other mutants in PRC2 components [27].

To test the H3K27me3 signal found in wild type and *fie* tiling arrays, we performed locus-specific qPCR on our ChIP-derived DNA-material. We analyzed seven gene loci and corroborated a H3K27me3 signal in wild type and its absence in *fie* (Figure S6A, S6D). Moreover, we could detect in qPCR experiments only a slight increase in H3K27me3 over heterochromatic regions in *fie* in contrast to the array signal (Figure S6A, S6E, S6F). In any case, the signal over heterochromatic regions was much below the level of H3K27me3-positive genic regions in wild type. These findings suggest that the antibody recognizes additional epitopes besides the H3K27me3 mark, preferentially in the absence of the proper antigen. A weak signal may get artificially enhanced in ChIP-on-chip experiments due to the global amplification procedure that is not applied in gene-specific ChIP-qPCR experiments.

To investigate the specificity of the antibody, we performed peptide competition assays. Nuclear protein extracts isolated from wild type showed a strong signal in Western blots while no band corresponding to the H3K27me3 mark could be detected in homozygous *fie* mutants under standard conditions (Figure 3A). However, when over-exposed or under less stringent conditions a faint signal also became visible in *fie* (Figure 3A, 3B). Using increasing peptide concentrations of up to 10 µg of H3K27me2 and H3K27me1 peptides, a gradual decrease in signal strength was observed in the case of H3K27me2 and H3K27me1 in the *fie* mutant, with the mono-methylated peptide being the most effective (Figure 3C). As the signal was strongly reduced by the

Table 1. Segregation analysis.

| Cross ³ | Genotype of the progeny in percent ^{1,2} | | | | | N ⁷ |
|---------------------------------|---|----------------|-------------------|-------------------|----------------------|----------------|
| | <i>FIE</i> -WT | <i>fie</i> +/– | <i>fie</i> –/– | <i>CDK</i> -WT | <i>cdk</i> +/– | |
| WT x <i>fie</i> | 50.0 | 50.0 | n.a. ⁴ | n.a. | n.a. | 40 |
| <i>fie</i> x WT | 100.0 | 0.0 | n.a. | n.a. | n.a. | 48 |
| <i>fie-cdk</i> x <i>fie</i> | 53.3±1.3 | 46.7±1.3 | 0.0 | n.d. ⁵ | n.d. | 448 |
| <i>fie</i> x <i>fie-cdk</i> | 28.8±4.6 | 62.4±3.2 | 8.8±2.4 | n.d. | n.d. | 757 |
| <i>fie-cdk</i> x <i>fie-cdk</i> | 35.2±10.1 | 58.0±9.0 | 6.8±1.6 | n.d. | n.d. | 428 |
| WT x <i>cdk</i> | n.a. | n.a. | n.a. | 91.1±0.8 | 8.9±0.8 ⁶ | 90 |
| <i>cdk</i> x WT | n.a. | n.a. | n.a. | 53.9±2.4 | 46.1±2.4 | 91 |
| <i>fie cdk</i> x <i>cdk</i> | n.d. | n.d. | n.a. | 34.4 | 65.6 | 32 |
| <i>cdk</i> x <i>fie cdk</i> | 51.5 | 48.4 | n.a. | 51.8 | 48.2 | 56 |

1 Genotypes are given in % of the total germinated seedlings.
 2 Standard deviation is given in case more than one individual cross has been analyzed.
 3 The female partner of the cross is always indicated first. Crosses have been performed with either wild type lines or plants heterozygous for *fie* and/or *cdka;1*, referred to as *fie* and *cdk*, respectively.
 4 n.a. = not applicable.
 5 n.d. = not determined.
 6 Consistent with previous studies, the transmission of *cdka;1* from the paternal side was found to be approximately 9% indicating successful wild-type like double fertilization. These cases of double fertilization would lead in crosses with *fie* as a female partner to over-proliferation of the endosperm and seed abort.
 7 Number of plants analyzed.
 doi:10.1371/journal.pgen.1002014.t001

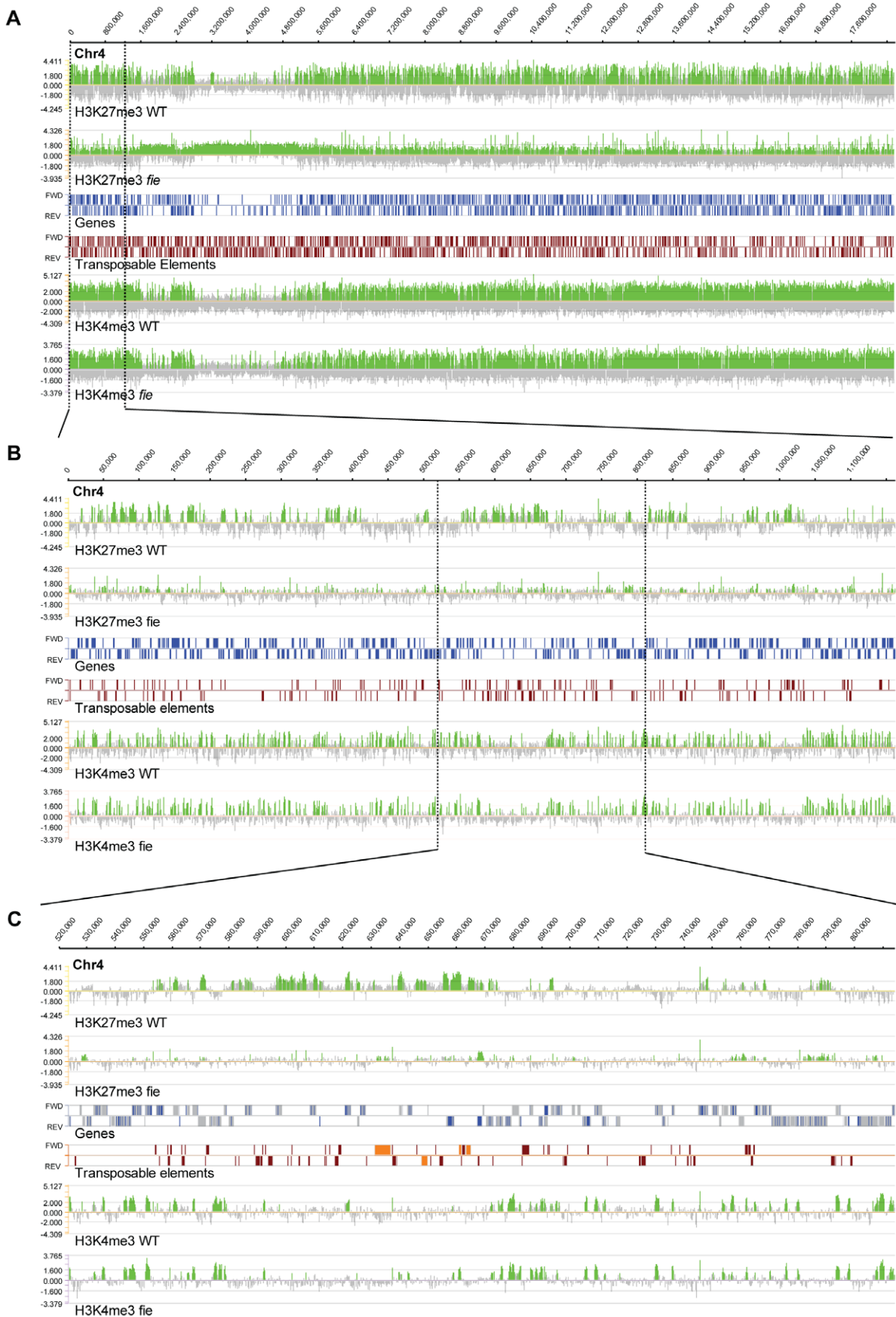


Figure 2. Genome-wide distribution of H3K27me3 and H3K4me3 marks. Genome browser view of Chromosome 4 with the H3K27me3 profile in wild type (first panel) and *fie* (second panel), boxed annotation of genes in blue (coding region) and grey (introns) (third row), boxed annotation of transposable elements and other heterochromatic regions in brown and orange (transposable element genes) (fourth row), the H3K4me3 profile in wild type (fifth panel) and in *fie* (sixth panel). Enrichment in H3K27me3 or H3K4me3 marks is shown in green bars. (B) and (C) are close-ups and show the major loss of H3K27me3 in *fie* whereas H3K4me3 distribution is basically unchanged. Raw data have been deposited at GEO database (GSE24163, <http://www.ncbi.nlm.nih.gov/geo/query/acc.cgi?acc=GSE24163>). doi:10.1371/journal.pgen.1002014.g002

peptides the cross-reactivity of the antibody might account to a large extent for the remaining H3K27me3 signal in our Western and ChIP-experiments. Moreover the H3K27me3-peptide could not deplete the signal further in *fie* as would be expected when the mutant is already largely devoid of any H3K27me3 (Figure 3B). In contrast, the trimethylated peptide effectively reduced the signal in wild type to a level comparable to the detection level in *fie* whereas the H3K27me2- and H3K27me1-peptides did not show any obvious effect in wild type samples up to concentrations of 10 μ g (Figure 3B, 3D). Thus, we conclude that the remaining signal in *fie* is not H3K27me3 but to some extent H3K27me2 and more pronounced H3K27me1 demonstrating a slight cross-reactivity of the antibody. Given that H3K27me1 is found mainly over heterochromatic regions in *Arabidopsis* wild-type plants [30], we conclude that a cross-reactivity of the H3K27me3 antibody with H3K27me1 accounts for the gain in signal over repeat-regions and transposable elements in the *fie* mutant.

Genes involved in plant reproduction are particularly up-regulated in homozygous *fie* mutant seedlings

To unravel the transcriptional consequences upon the loss of PRC2 function we compared genome-wide expression levels of homozygous *fie* mutants with wild type at two different time points. At 7 DAS, no major transformations were observed, yet the plants could be unambiguously and reproducibly identified as homozygous *fie* mutant plants due to their aberrant root growth and subsequent genotyping (Figure 1). At the second time point at 20 DAS, substantial morphological transformations were clearly visible.

Within our reference set (Table S3), a total of 1115 genes were significantly up-regulated at 7 DAS and 1735 genes at 20 DAS in *fie* versus wild-type plants (Bonferroni P-value ≤ 0.05 , see Material and Methods). Conversely, we also found genes to be significantly weaker expressed in *fie* versus wild type: 1308 and 1843 genes at 7 DAS and 20 DAS, respectively (Bonferroni P-value ≤ 0.05 ; Figure S7). Next, we compared the expression data with our PRC2 target gene set. Only a fraction of all identified PRC2 target genes became up-regulated in *fie* mutants, indicating that PRC2 is not the only repressive system and/or besides the revelation of the repression activators are required for gene expression (Figure S7). Still, our data are consistent with the concept that H3K27me3 mark is associated with inhibition of gene expression since the overlap of the group of up-regulated genes at 7 DAS and 20 DAS with the group of H3K27me3 marked genes is larger than expected by random (7 DAS and 20 DAS: representation factor (rf) = 7.1, $p < 1.0e-99$ *; 7 DAS and H3K27me3: rf = 1.6, $p < 1.8e-21$; 20 DAS and H3K27me3: rf = 1.1, $p < 0.009$; Figure S7). Conversely, for down-regulated genes at 7 DAS we see the opposite effect, i.e. the overlap of both gene sets is smaller than expected at random (7 DAS and 20 DAS: rf = 7.5, $p < 1.0e-99$; 7 DAS and H3K27me3: rf = 0.6, $p < 1.3e-13$; 20 DAS and H3K27me3: rf = 0.9, $p < 0.122$; Figure S7).

To evaluate the PRC2 targets that are up-regulated, potentially in direct response to the loss of H3K27me3, we examined which gene ontology (GO) categories are overrepresented among the up-regulated genes that lost H3K27me3 in *fie* mutants using the

BINGO analysis software [31]. Most overrepresented GO categories in the classification system *biological function* relate to reproduction with two distinct subcategories: Flower- and seed development (Figure 4, Figure S8). Besides reproduction, a few additional small categories were overrepresented such as abscisic acid (ABA) signaling and lipid-transport and -sequestering. However, a closer analysis of the corresponding genes revealed that they are also linked with reproduction, in particular seed development (see below).

PRC2 function in flower and seed development

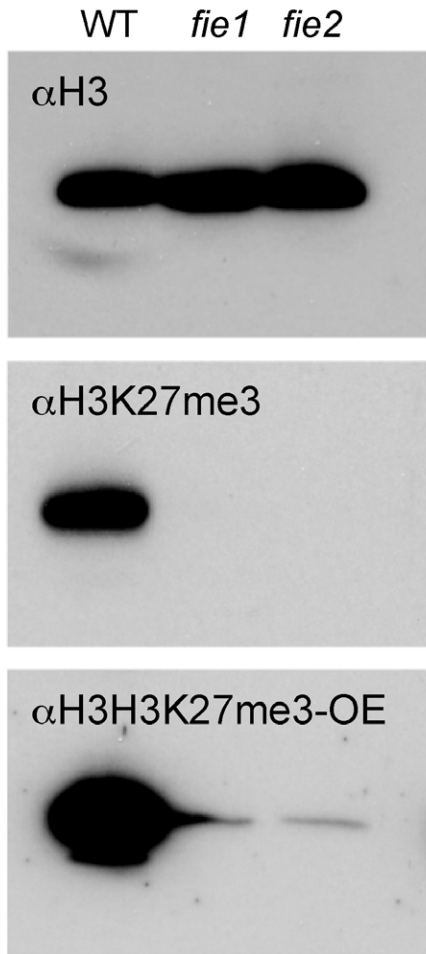
H3K27me3 appears to be a key repressive mechanism for the expression of many genes controlling different aspects of flower development and consistent with this, homozygous *fie* mutants are very early flowering, i.e. as early as 10 DAS and produce ectopical flowers, e.g. on roots. A similar early flowering phenotype has been found in mutants with compromised PRC2 activity [5,6,32], and has been related to the early deregulation of LEAFY (LFY), AGAMOUS (AG) and PISTILLATA (PI), which starts as early as the embryonic stage. Our analysis identifies several additional genes controlling flower development as PRC2 targets that are significantly up-regulated in *fie* mutants, including genes involved in the establishment of a floral meristem (e.g. *FLC*, *AGL24*, *LFY*, *FUL* and *CAL*), genes involved in promoting a determinate floral meristem (e.g. *ULT1*, *PAN*, *LFY*) and genes involved in organ identity specification (e.g. *AP3*, *SEP3*, *LFY*, *PI*) (Figure S9). The results of our microarray experiments could be validated by qRT PCRs confirming the significant up-regulation of 5 genes (*AP3*, *CRC*, *FLC*, *PI*, *SEP3*). In addition, 2 genes that were only slightly (but not significantly) up-regulated in our microarray experiment were also found to have significantly elevated expression levels in the qRT PCR on *fie* mutant material (*AG*, *API*), whereas the flowering regulator *FWA* shows neither upregulation in the array nor in qRT-PCR experiments (Table S4).

The second principal category of PRC2 target genes that became up-regulated in *fie* mutants are genes functioning in late seed development (Figure 4, Figure S8, Figure S10). Among the PRC2 targets that are up-regulated in *fie* we find genes acting at different hierarchical levels in late seed development, from master regulators (e.g. *AGL15*, *LEC2*, *ABI3*, *FUS3*) and more specific modulators (e.g. *WRI*, *FLC*) over genes promoting ABA and/or inhibiting GA signaling (e.g. *ABI4*, *DOG1*, *CHO1*, *SOM*, *SPL8*) down to target genes such as storage compounds (e.g. *CRU3*, *CRA1*, *LEAs*, *oleosins*) (Figure 5).

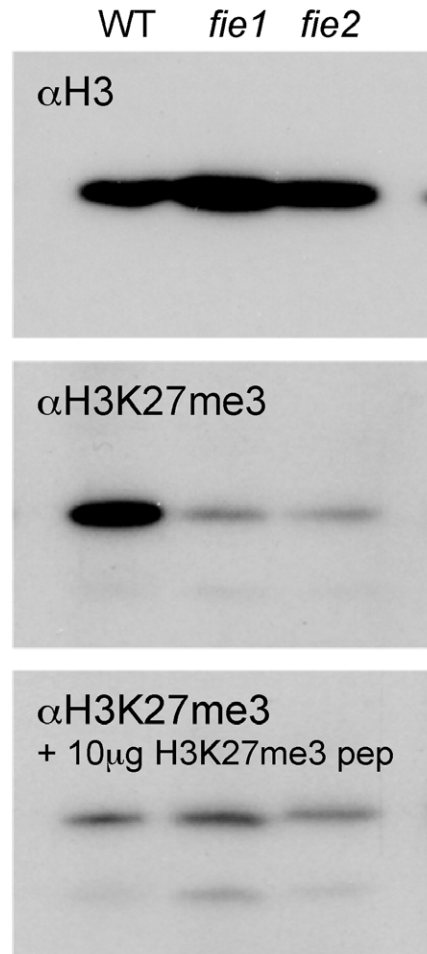
The up-regulation of many important seed regulatory genes raised the hypothesis that *fie* seedlings, albeit macroscopically resembling wild type seedlings, display seed phase characteristics. To test this, we first analyzed the lipid content using the dye *Fat Red* that stains for triacylglycerol-lipids in red color. Whereas wild-type seedlings displayed a sharply decreasing lipid content from 5 to 8 DAS, *fie* mutants showed an intense red color indicating a high lipid content that is typical for late seed maturation stages in wild type (Figure 1M, 1N).

To test whether the failure to repress late seed genes during the seed maturation process interferes with germination, we performed seed germination assays of *clf-swn* and *fie* mutants in

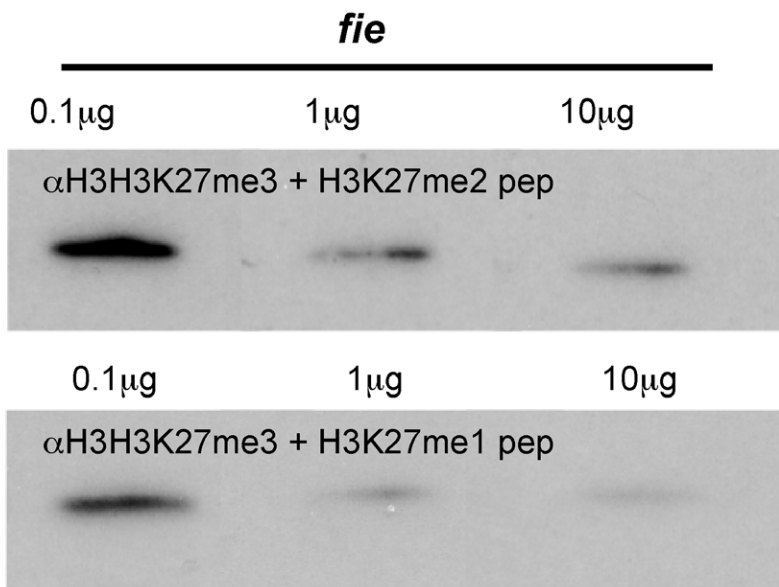
A



B



C



D

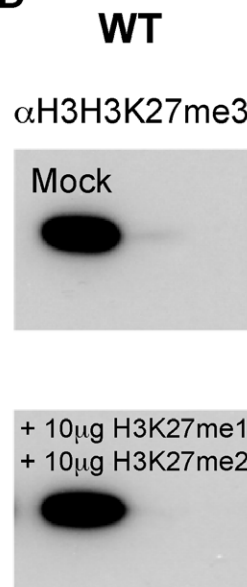


Figure 3. Western blot detection of the H3K27me3 mark. Western blot analysis of H3K27me3 in wild type and *fie* mutants. (A) Comparison between wild type and *fie* nuclear extracts revealed major loss of H3K27me3-signal in the mutant; however, after over-exposure (OE) a faint signal becomes visible in *fie* mutants. Detection of histone H3 was used as a loading control. (B) Under less stringent conditions a weak signal in *fie* is detectable by the H3K27me3 antibody. Pre-incubating the antibody with a surplus of H3K27me3 peptides, reduces the signal intensity to only of faint band in wild-type extracts that roughly matches the intensity of the remaining signal seen in *fie* mutants. Detection of histone H3 was used as loading control. (C) Peptide competition assay using H3K27me3 antibody with increasing concentrations of H3K27me1- and H3K27me2-peptide in *fie* mutant resulted in a strong reduction of the remaining signal detected by the H3K27me3 antibody. (D) Both peptides could not reduce the H3K27me3 signal in wild-type extract indicating that the antibody works properly given that sufficient antigen is provided.
doi:10.1371/journal.pgen.1002014.g003

comparison with wild-type plants. Whereas all wild-type seeds germinated within 2 DAS, both *clf-swn* and *fie* mutants show delayed germination (Figure 6A). Eventually, over 90% of *clf-swn* mutants germinated around 4 DAS. In contrast, approximately 40 percent of the homozygous *fie* mutants stayed dormant for the course of the entire experiment (20 days), as revealed by dissecting dormant seeds and genotyping of the embryos.

Dissected dormant embryos were then allowed to develop on agar plates. As a reference wild-type embryos were isolated from seeds 24h after imbibition. Initially, dormant *fie* embryos are indistinguishable from wild type embryos (Figure 6C, 6F) and around 1/4 of these *fie* mutants started to develop in a similar

manner as wild type, showing root- and root hair formation, unfolding and greening of the cotyledons and the accumulation of anthocyanin (Figure 6C–6H). However the remaining 3/4 of *fie* embryos stayed dormant for a period of several days. Some of these finally could break dormancy and started to develop although proliferation was extremely delayed (Figure 6L–6N). Notably, heterozygous *cdka;1* mutants behaved like wild type seeds consistent with the previous finding that *cdka;1* mutants are sporophytically recessive. Similarly, double heterozygous *cdka;1-fie* mutants also did not show any germination defects demonstrating that the observed dormancy phenotypes are due to the loss of PRC2 function.

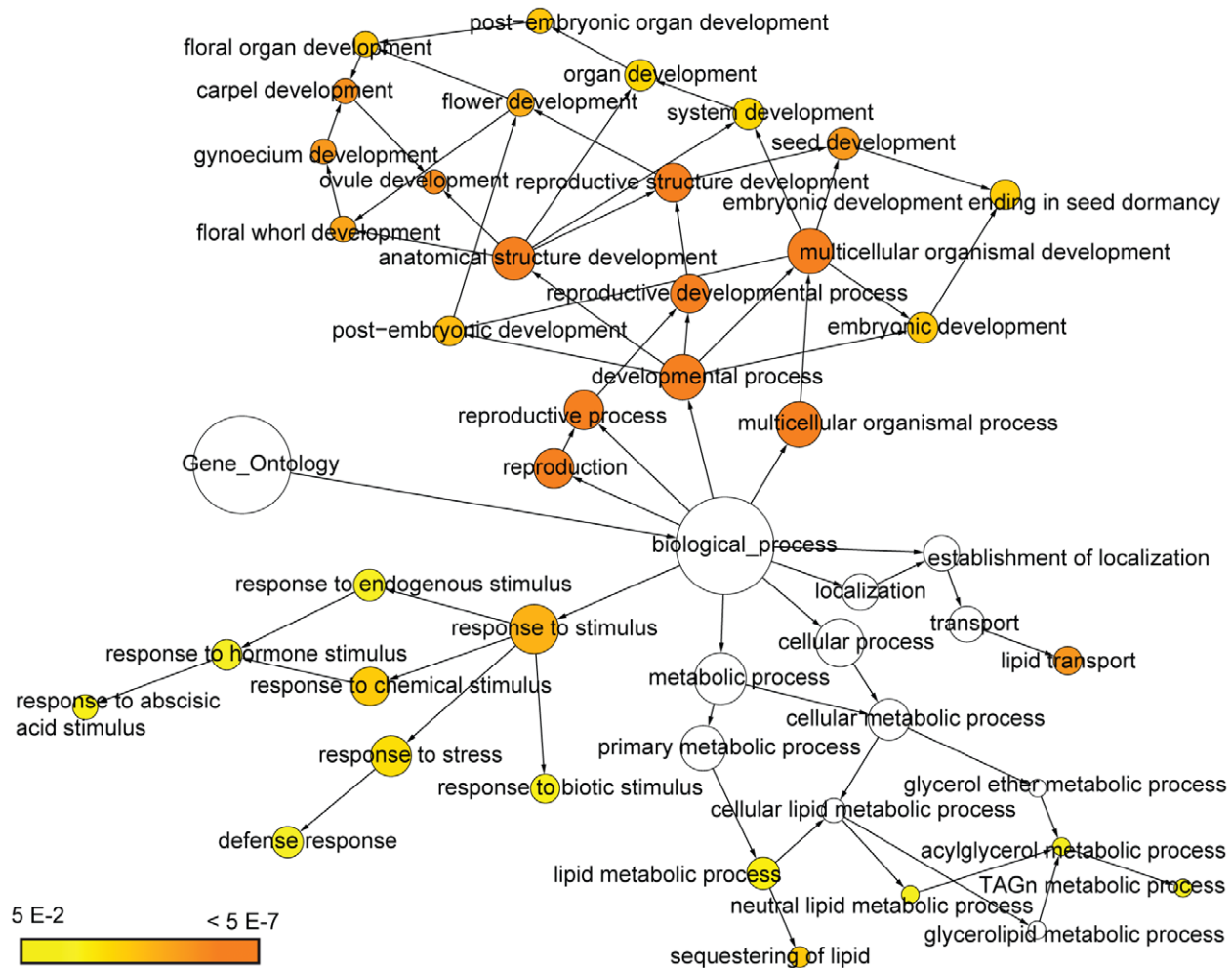


Figure 4. Overrepresented gene ontology categories in the set of H3K27me3 targets that are up-regulated in *fie*. BiNGO (the Biological Network Gene Ontology tool) analysis representing over-represented categories of the ontology *Biological Process* among the genes that are marked by H3K27me3 in the wild type (20 DAS) and are significantly up-regulated in 7 DAS *fie* mutant seedlings. The size of the nodes is proportional to the number of genes in the test set which are annotated to that node. Colored nodes are significantly over-represented, with a color scale ranging from yellow (p -value = 0.05) to dark orange (p -value = 5.00×10^{-7}). Statistical testing was as described by Maere et al. (2005) [31].
doi:10.1371/journal.pgen.1002014.g004

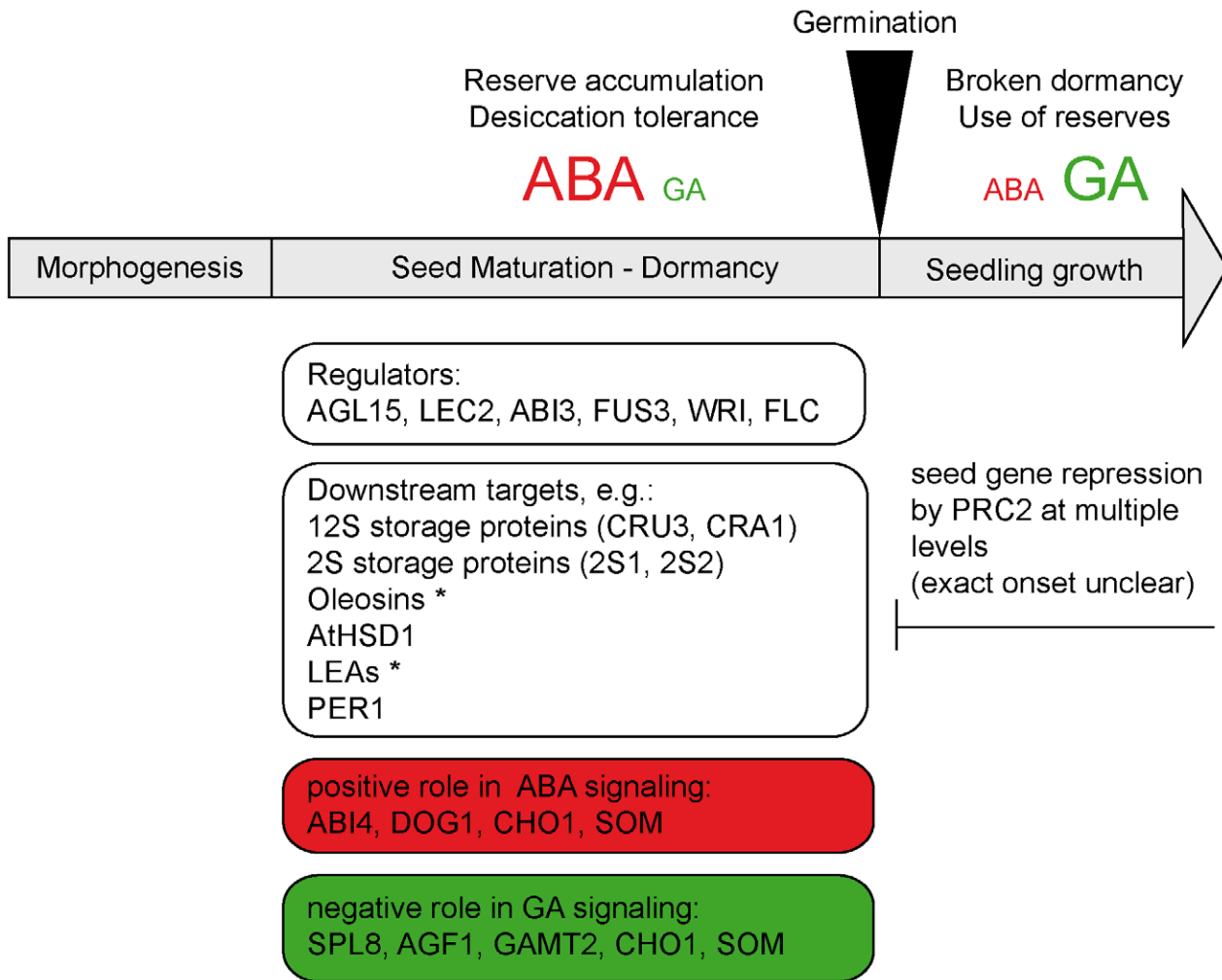


Figure 5. PRC2 represses seed maturation and dormancy genes in the seedling. All genes provided in this model have been identified as H3K27me3 targets and were significantly up-regulated in *fie* mutants. They include master regulators of seed development such as *AGL15*, *LEC2*, *ABI3*, *FUS3*, further downstream regulators such as *WRI*, integrators of environmental signals such as *FLC* and finally genes involved in seed storage and desiccation tolerance. * For detailed information which members of the oleosins (oil body coat proteins) and LEAs (late embryogenesis abundant proteins) are affected see Table S5. For *LEC2* the up-regulation was only observed in qRT-PCR (Table S4). We find here that the ABA and GA hormonal signaling pathways that play a pivotal role in the transition from seed to seedling are under PRC2 control since genes playing a positive role in ABA signaling as well as genes with a negative role in GA signaling are H3K27me3 marked in wild type and up-regulated in *fie*. Large letters stand for high and small for low ABA and GA levels, respectively. Abscisic acid (ABA), Gibberellic acid (GA), AGAMOUS-Like 15 (*AGL15*, AT5G13790), LEAFY COTYLEDON 2 (*LEC2*, AT1G28300), ABA INSENSITIVE 3 (*ABI3*, AT3G24650), FUSCA 3 (*FUS3*, AT3G26790), WRINKLED1 (*WRI*, AT3G54320), FLOWERING LOCUS C (*FLC*, AT5G10140), CRUCIFERIN 3 (*CRU3*, AT4G28520), CRUCIFERINA (*CRA1*, AT5G44120), SEED STORAGE ALBUMIN 1 (2S1, AT4G27140), SEED STORAGE ALBUMIN 2, (2S2, AT4G27150), HYDROXYSTEROID DEHYDROGENASE 1 (*AtHSD1*, AT5G50600), Peroxiredoxin 1 (*PER1*, AT1G48130), ABA INSENSITIVE 4 (*ABI4*, AT2G40220), DELAY OF GERMINATION 1 (*DOG1*, AT5G45830), CHOTTO 1/AINTEGUMENTA-LIKE 5 (*CHO1/AIL5*, AT5G5739), SOMNUS (*SOM*, AT1G03790), SQUAMOSA PROMOTER BINDING PROTEIN-LIKE 8 (*SPL8*, AT1G02065), AT-hook protein of GA feedback 1 (*AGF1*, AT4G35390), GIBBERELIC ACID METHYLTRANSFERASE 2 (*GAMT2*, AT5G56300). doi:10.1371/journal.pgen.1002014.g005

Germination is associated with a low ABA to gibberellic acid (GA) ratio [1]. Intriguingly, the development of some of the dissected, initially dormant *fie* seedlings resembled the development of wild-type plants that germinated on high concentration of ABA, lacking proper greening of aerial tissue, root formation and expansion of true leaves (Figure 7I–7J, 7L–7M). However, applying high dosage of GA did not lead to higher germination rates of *fie* mutants (Figure 7B), suggesting that the primary defect in the class of non-germinating *fie* seeds is dormancy release and not the germination itself.

Overrepresentation of PRC2 target genes in particular gene families

Among the up-regulated genes in *fie* controlling seed and flower development certain gene families appeared to be overrepresent-

ed, e.g. transcription factors, consistent with previous studies showing that those are in particular marked by H3K27me3 (Table 2) [7,29,33]. To get a more detailed picture, we tested whether all transcription factor families are equally subject to regulation by PRC2 (Figure S11A, S11B). Approximately 2/3 of all transcription factor families have members that are marked by H3K27me3 at 20 DAS. Notably, one of the largest transcription factor families within our reference set in which none of the member was found to carry H3K27me3 was the group of AUXIN RESPONSIVE FACTORS (ARFs) that mediate auxin signaling (Table S3). However, at a more general level, we found that other genes involved in the auxin signal transduction network are targets of PRC2 regulation, for instance several IAAs and PIN auxin transport facilitators (Table S1).

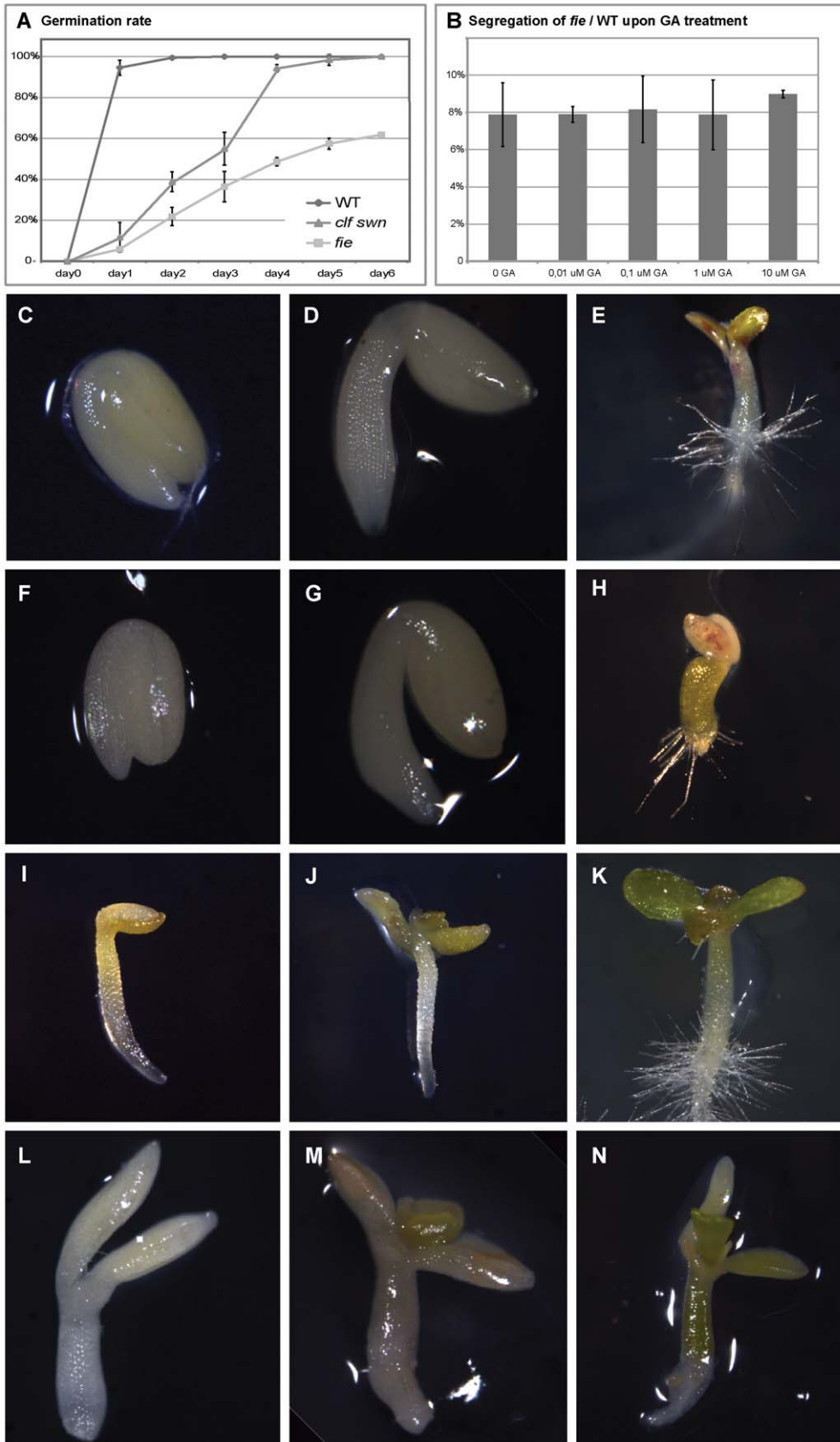


Figure 6. Dormancy and germination phenotypes. (A) Both, homozygous *fie* and homozygous *clf-swn* mutants, show a similar delay in germination initially. However, *clf swn* germinates to 100% whereas 40% of *fie* seeds stay dormant within at least two weeks on plates. (B) Application of GA does not enhance the germination rate of *fie* mutant seeds. (C–N) Phenotypical comparison of wild type (C–E, I–K) and *fie* mutants (F–H, L–N).

(C–H) Time series of post-embryonic development for dissected wild type (C–E) and *fie* (F–H) till day 3 after isolation. Initially, *fie* embryos isolated from dormant seeds (F) are undistinguishable from wild type embryos dissected 24h after imbibition (C). (D) Wild type embryos start to grow within 24h after the transfer to media. (E) Unfolding as well as greening of the cotyledons, root growth and root hair formation as well as anthocyanin accumulation takes place within 3 days. (G–H) Around ¼ of the *fie* seedlings break dormancy and display a similar developmental program as wild type from day 1 (G) to day 3 (H) after dissection. (I–K) Effect of ABA on wild type seedling growth. (I, J) Wild-type seedlings germinated on ABA-containing media are strongly affected in growth, appear yellowish, are delayed in greening and do not produce roots. (K) After the transfer from ABA plates to normal media, wild-type plants recover within 24h, e.g. they green, and show completely normal development further on. (L–N) The majority (around ¾) of the dissected *fie* mutant embryos do not develop similar to wild type, but resemble wild type plants germinated on high levels of exogenous ABA. (M,N) Typically, a strong delay in growth and greening with yellowish cotyledons and defects in root- and root hair growth and stunted leaves is observed, though the overall body plan is not affected (N) Greening is seen only after 10 days. (L) In some cases the mutant does not develop seedling traits at all.
doi:10.1371/journal.pgen.1002014.g006

Among transcription factor families that are marked with H3K27me3, the fraction of PRC2 targets varies substantially. A particular high proportion of PRC2 targets (≥60%) were found in MIKC subclass of MADS transcription factors, in the WOX-class, the HD-Zip-IV Homeobox class and in the C2C2-Dof and C2C2-YABBY zinc finger classes, for the latter even all 6 members were found to be PRC2 targets. The transcription factor subfamily with

the most (in absolute numbers as well as in percentages) PRC2 targets that also showed transcriptional up-regulation in *fie* is the MIKC class, among which we find central regulators of seed and flower development (Figure S11, Table S1, Table S5) [34].

In addition to transcription factors, a few other gene families were overrepresented among the PRC2 targets that are up-regulated in *fie*; the most prominent are oleosins and LATE

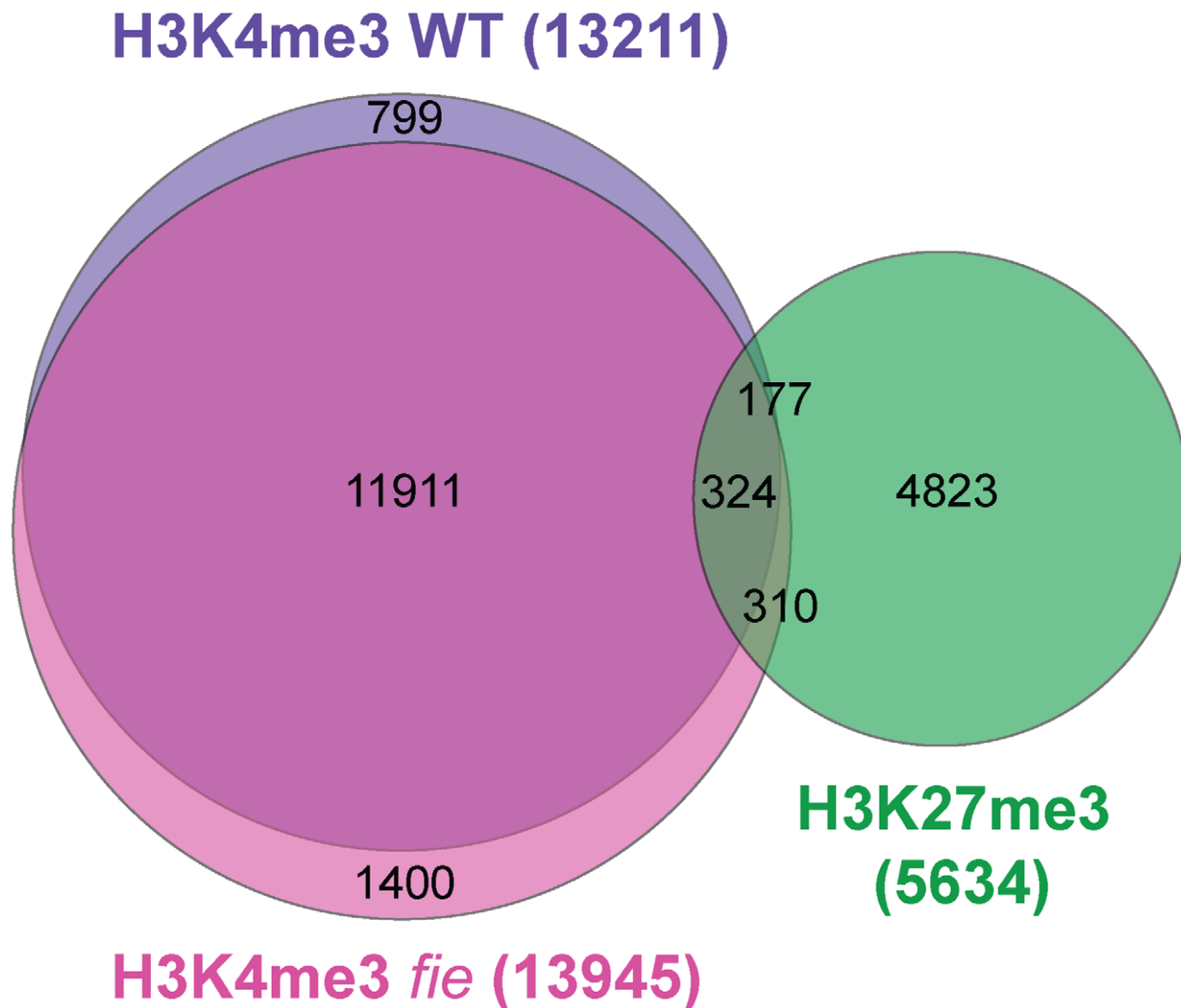


Figure 7. The set of H3K4 trimethylated genes changes only marginally between wild type and *fie* and is under-represented among H3K27me3 targets. VENN Diagram representing the number of genes marked by H3K27me3 in wild type (green) and H3K4me3 in wild type (purple) and *fie* (pink). The mutual overlap of the H3K4me3 targets in wild type and *fie* is larger than expected for two independent sets, while the overlap of the H3K4me3 marked genes with the H3K27me3 marked genes is significantly smaller (wild type H3K4me3 and *fie* H3K4me3: $r_f = 1.9$, $p < 1.0e-99^*$; wild type H3K4me3 and wild type H3K27me3: $r_f = 0.2$, $p < 1.0e-99^*$; *fie* H3K4me3 and wild type H3K27me3: $r_f = 0.2$, $p < 1.0e-99^*$). P-values marked by an asterisk (*) were below the calculation limits of the software (highly significant).
doi:10.1371/journal.pgen.1002014.g007

Table 2. Overrepresentation of in wild-type H3K27me3 marked and in *fie* up-regulated genes in specific gene classes.

| | All | TF | MADS | MIKC | LEAs | Oleosins |
|--------------------------------------|-------|-------|-------|-------|-------|----------|
| Total | | 1839 | 108 | 39 | 56 | 18 |
| In reference set (= 100%) | 24901 | 1771 | 91 | 37 | 54 | 17 |
| H3K27me3 WT | 20.8% | 34.4% | 60.4% | 86.5% | 50.0% | 64.7% |
| Down in <i>fie</i> | 9.7% | 8.4% | 1.1% | 2.7% | 11.1% | 0.0% |
| Up in <i>fie</i> | 9.2% | 9.9% | 19.8% | 40.5% | 44.4% | 70.6% |
| Up in <i>fie</i>, H3K27me3 WT | 2.2% | 4.1% | 16.5% | 40.5% | 29.6% | 47.1% |

The percentage of H3K27me3 marked and/or deregulated genes is shown for the entire reference set (column All) and different subgroups of genes, namely transcription factors (TF), family of MADS transcription factors (MADS), subfamily of MADS-MIKC transcription factors (MIKC), family of late embryogenesis abundant proteins (LEAs), family of oil body coat proteins (oleosins).

doi:10.1371/journal.pgen.1002014.t002

EMBRYONIC ABUNDANT PROTEIN genes (LEAs). Oleosins are structural components of oil bodies and were found to be expressed preferentially in seeds or the tapetum layer of developing anthers [35] (Figure 5, Table S5). 11 of the 17 oleosin genes in our reference set are H3K27me3-marked and 8 are in addition up-regulated in *fie* (Table 2), which matches the observation of storage lipid accumulation in *fie* (Figure 1M, 1N). This is a strong overrepresentation since from all genes in our reference set, we find not more than 21% marked by H3K27me3 and only 2% being up-regulated in *fie* as well.

Another gene family that is highly overrepresented in the class of up-regulated PRC2-targets are LEAs, most of which are expressed in seeds. Of 54 LEAs covered by our reference set, we find 27 (50%) H3K27me3-marked and 16 (30%) being in addition up-regulated in *fie*. Interestingly, we found 7 (13%) of the LEAs down-regulated in *fie* and with a single exception these are not H3K27me3 targets and show a non-seed specific expression (Table S5, Figure S10) [36,37].

Crosstalk in chromatin regulation

In *Drosophila* the function of the Polycomb complex Group (PcG) is counteracted by the action of the trithorax Group (trxG) [7]. In *Arabidopsis*, the role of TRX has been assigned to ATX1, ATXR7/SET DOMAIN GROUP25 (SDG25), PICKLE (PKL)/PICKLE-

Table 3. The percentage of up-regulated genes in *fie* mutants is positively correlated with loss of H3K27me3 and gain in H3K4me3.

| | Reference set | Up in <i>fie</i> , 7 DAS (% of reference) | Up in <i>fie</i> , 20 DAS (% of reference) |
|---|---------------|---|--|
| All | 24901 | 4.5 | 7.0 |
| Loss H3K27me3 in <i>fie</i> | 5175 | 7.0 | 7.7 |
| Gain H3K4me3 in <i>fie</i> | 1613 | 12.9 | 14.7 |
| Loss H3K27me3 and gain H3K4me3 in <i>fie</i> | 296 | 28.0 | 27.7 |

doi:10.1371/journal.pgen.1002014.t003

RELATED 2 (PKR2) and ULTRAPETALA 1 (ULT1) [38–42]. Our data showed that *ULT1*, *ULT2* and *PKR2* are PRC2 targets and at least *ULT1* and *ULT2* were substantially up-regulated at 7 and 20 DAS (Table S3). *ULT1* has been shown to act as an anti-repressor (i.e. limiting H3K27me3 deposition) and as an activator of the flower regulator *AG* by mediating Lysine 4 H3 trimethylation [42]. To test whether the loss of H3K27me3 is accompanied with a gain in H3K4me3, as suggested by our finding of a possible negative feedback of PRC2 on *ULT1/ULT2* activation, we analyzed the genome-wide distribution of H3K4me3 in wild type and *fie*.

Consistent with previous studies [43], we found that in wild-type plants a large number of genes (approximately 1/3 of the genome) are marked with H3K4me3 at 20 DAS (Figure 2, Figure 7). However, the number of genes that are marked by both H3K27me3 and H3K4me3 is significantly smaller than expected for an independent distribution, as was observed previously [43] (Figure 7). This indicates repulsion of these two marks in accordance with the model that H3K27me3 and H3K4me3 signifies repressed and activated genes, respectively. None-the-less, a small set of 501 genes was identified as marked by both histone modifications.

In our ChIP-chip experiments we found only a slight increase in number of genes that carry the H3K4me3 mark in *fie* in comparison to wild-type plants (13945 vs. 13211 genes) and we do not see an elevated level of H3K4me3 in Western blot analyses (Figure S6C). Thus, genes that lose H3K27me3 do not in general gain H3K4me3 in *fie* (Figure 7, Table S3). On the other hand, gene up-regulation in *fie* is positively correlated with loss of H3K27me3 and gain in H3K4me3. The global proportion of genes with elevated expression in *fie* at 7 DAS is 4.5% while the percentage of up-regulated genes reaches 28% amongst those that lose H3K27me3 and concomitantly gain H3K4me3 (Table 3). In addition, for certain gene families, such as the MIKC group of MADS transcription factors, the WOX group of Homeobox genes and the oleosins, we find those genes that gain H3K4me3 in addition to the loss of H3K27me3 to be among the most highly up-regulated for these specific classes (Table 3, Table S5).

Thus, our data supports the view that H3K4me3 and H3K27me3 are mutually exclusive marks though in general a loss in H3K27me3 is not sufficient to gain H3K4me3. However, a tightly linked interdependency between both antagonistic marks is operating for a relatively small group of genes including members of the MIKC class of major developmental regulators [42,44,45]. Our finding that the PRC2-antagonizing TRX-function genes *ULT1/ULT2* are themselves targets of PRC2 and consequently up-regulated in *fie*, provides a possibility for the molecular implementation of such an interconnected control mechanism.

Discussion

Here we have generated homozygous *fie* mutant plants overcoming a block in the analysis of PRC2 activity in the flowering plant *Arabidopsis*. Our approach relies on bypassing of double fertilization and circumventing the requirement for FIE during endosperm development. This has allowed us to study the genomic and developmental consequences of the complete loss of PRC2 activity during embryo and subsequent sporophyte development.

Genomic perspective

Several lines of evidence indicate that PRC2 in plants is indeed essential for depositing H3K27me3 marks similar to its function in animals. First, our ChIP-on-chip experiments showed that there is no or only a very weak H3K27me3 signal in *fie* and that the remaining signal shows properties that differ from the typical H3K27me3 mark. Second, at least 3 heterochromatic regions that

showed H3K27me3 signal in *fie* in ChIP-on-chip experiments did not show a substantial level of enrichment in gene specific ChIP-qPCR assays. Third, the little residual signal of H3K27me3 in *fie* mutants can be further reduced in peptide competition assays with peptides that harbor H3K27me2 or H3K27me1 epitopes. Finally, H3K27me3 peptide is not effective in reducing the signal in *fie* further, as would be expected when the remaining signal were H3K27me3. Conversely, the H3K27me3 peptide could reduce the antibody signal in wild type to the signal strength found in *fie*.

Based on the by large mutually exclusive distribution of H3K27me3 and H3K4me3, we asked if genes which lost H3K27me3 in *fie* would in turn acquire H3K4me3. Such a reciprocal regulation has been found for *AG* and *FLC* in *Arabidopsis* [42,44,45]. Indeed, we could confirm that *AG* and *FLC*, both members of the MIKC transcription factor class, gain H3K4me3 in the absence of *FIE*. Moreover, 7 other MIKC transcription factors that represent important regulators during development showed a similar response. It was recently shown that the SAND domain protein ULTRAPETALA1 (*ULT1*) mediates the switch from H3K27me3 to H3K4me3 at the *AG* locus [42]. Interestingly, we found that *ULT1* itself is under the control of PRC2, as it is marked by H3K27me3 in wild type and shows strong up-regulation in *fie*. This might explain the switch from H3K27me3 to H3K4me3 as seen for a remarkable number of the MIKC transcription factors. In animals the maintenance of trimethylated H3K4 was shown to require permanent TRX activity to counteract PRC2, as the repressive H3K27me3 state seems to be the default state for genes that are regulated by both antagonizing HMTase machineries [9]. However, global changes in H3K4me3 levels were not observed in *fie*, and the change from H3K27me3 to H3K4me3 was restricted to about 5.5% of the genes marked by H3K27me3.

We also identified a small group of potentially bivalently labeled genes (1.8% of reference set), i.e. harboring the activating H3K4me3 and the repressive H3K27me3 mark. The concomitance of both tags is found in more than 10% of all genes in human and mouse embryonic stem cells and *Xenopus tropicalis* embryos, and is thought to maintain the target genes in a “poised state”, resulting in transcriptional silencing but allowing for fast reactivation upon commitment to differentiation [46–50]. Bivalency has to our knowledge only been found for the *AG* and *FT* loci in *Arabidopsis* and its existence is also unclear for *Drosophila* [44,51,52]. However, we showed here that in contrast to *Drosophila* and mouse, *Arabidopsis* does not require the PRC2 to establish a normal body organization (see below). This renders it unlikely that animals and plants are using the same epigenetic mechanisms to set up the body plan, at least during embryogenesis.

Developmental perspective

The observation that the plant body plan can be established without PRC2 function is an unexpected result not only because PRC2 function is essential in animal embryogenesis but also regarding the strong postembryonic phenotype of *clf-swn* double mutants or *fie* mutants with a partially complementing *FIE* transgene [5,6]. The overall correct body plan of *fie* embryos and early seedlings suggests that there is a tight network of intercellular communication presumably maintaining positional cues in the plant embryo. Indeed, research in the last decade has unraveled several patterning mechanisms in the plant embryo, for instance polar auxin distribution and non-cell-autonomously acting transcription factors [53,54].

However, after body-plan formation, PRC2 function is key for the correct phase transition from embryonic to vegetative growth. Much

progress has been made in the understanding of chromatin regulation and in particular the function of PRC2 during the phase transition from vegetative growth to flowering (for review see [55–57]). In contrast, the view that chromatin regulation is important for controlling the switch from mature seed to seedling is only now emerging (for review see [58,59]), and the involvement of PRC2 in late seed development has been unclear beyond the finding that many genes implicated in seed maturation are labeled by H3K27me3 (for review see [58,60,61]). Defining the role of PRC2 during seed maturation has been obscured due to a prominent function of PRC2 earlier in seed development, i.e. for endosperm growth and differentiation. The combination of our genetics and genomics studies demonstrate that PRC2 is one of the major control systems of this phase change by shutting down the entire cascade of maturation genes from master regulators to a wide range of downstream targets before or at germination (see Figure 5). Moreover, our data suggest that the PRC2 mediated phase transition from seed- to seedling stage takes place primarily at the level of the embryo, as seeds with homozygous *fie* mutant endosperm but heterozygous mutant embryo germinate like wild type.

A wealth of genetic and physiological experiments has demonstrated that seed development is under the tight control of plant hormones and that GA triggers while ABA inhibits seed germination (for review see [1]). High ABA and low GA levels are characteristic for maturing seeds allowing the establishment of seed dormancy, while this relationship is inverted at germination. PRC2 action in the maturing seed seems to sustain the antagonistic action of the two plant hormones ABA and GA by inhibiting positive regulators in ABA and negative players in GA signaling. For example, the PRC2 target *SOMNUS* (*SOM*), a C2H2-type zinc finger protein, down-regulates GA and up-regulates ABA levels. *SOM* expression is seed specific and our finding that it is a PRC2 target and up-regulated in *fie* suggests that in wild type down-regulation of *SOM* is maintained by H3K27me3 to allow for high GA and low ABA levels in the germinating seed.

Besides the regulation of the ABA-GA signaling pathway, we also found that *DELAY OF GERMINATION 1* (*DOG1*), a major regulator of seed dormancy [62], is a H3K27me3 target and significantly up-regulated in *fie* seedlings. Interestingly, it was recently shown that *DOG1* is also regulated by *HISTONE MONOUBIQUITINATION1* (*HUB1*), a C2H2 RING finger protein required for histone H2B monoubiquitination [63].

In this context it will be interesting to examine if dormancy control is generally regulated at the level of chromatin, as for example different *Arabidopsis* accessions from diverse environmental origins show dramatic differences in seed dormancy [64]. Since PRC2 function in the perception of cold via the repression of the flowering inhibitor *FLC* is well established for the transition to the generative phase [57], it is tempting to speculate that a similar mechanism functions to perceive this environmental stimulus in the seed. The need of cold stratification in order to break seed dormancy in many plant species [65] and the observation that *FLC* plays a role in this process as well [66], might reveal a common regulatory mechanism operating in the transition from vegetative to generative phase as well as from embryonic to vegetative phase.

Interestingly another phase transition, the switch from gametophytic to sporophytic development was recently shown to be regulated by PRC2 in moss, where PRC2 represses the differentiation of the sporophyte [67,68]. The authors correlate their observations with the transition from gametophytic to sporophytic development in flowering plants that is as well controlled by PRC2, as *Arabidopsis fie* mutants for example show untimely development of the gametophytic endosperm without fertilization [22,67,69,70].

The reprogramming of gene activity is a mandatory step to allow for cellular differentiation processes and the stable inheritance of these differentiation states needs to be maintained for the integrity of the organism. Plants in particular have to adapt to environmental conditions and therefore need to change their developmental phase accordingly, and the phase transition from embryo to seedling stage can be considered as the earliest adaptive phase in plants. The origin of seed dormancy in land plant evolution is regarded as a major step in the successful establishment of flowering plants to sustain in non-favorable conditions and its control by PRC2 is an exciting example for the recruitment of an evolutionary conserved molecular machinery to fulfill new functions.

Material and Methods

Plant material and growth conditions

Unless indicated otherwise, Col-0 was used as wild type for all experiments. The *cdka;1-1* (AT3G48750) allele has been previously described (SALK_106809 [22]). The SALK_042962 line was used as the standard allele for *fie*. As additional *fie* alleles the T-DNA lines GK-362D08-016994 and GK-534F01-020364 were used that both displayed the previously described typical *fie* mutant phenotype. One previously described *fie* allele in WS-0 [71] was sequenced and shown to carry a base-pair exchange mutation 5' of the fourth splice acceptor site. The *curly leaf* (*clf-28*, SALK_139371, At2g23380) and *swinger* (*swn-4*, SALK_109121, At4g02020) alleles have been previously described [72,73]. All seeds were sterilized using chloride gas and sown on 0.8% Phyto agar plates (1/2 Murashige & Skoog (MS) salts and 1% sucrose) and grown under day neutral conditions (12h light 21°C, 12 h dark 17°C). After germination, plants were transferred to either new plates for long-term observation or to soil and grown in long day conditions (16 h, 22°C light; 8 h, 18°C dark).

Germination assays and hormone treatment

To examine germination, seeds from plants that were grown under the same growth conditions and stored for at least 3 months were sterilized with Chloride-gas and stratified for at least 4 days at 4°C. Upon germination induction (light, 21°C), germination rate was monitored for the following 6 days. After approximately 14 days the plants were analyzed with respect to their phenotype to distinguish between mutants and phenotypically wild-type plants and correlated with the day of germination. Dormant seeds were dissected under a stereomicroscope using a fine needle and fine forceps and subsequently genotyped by PCR. Gibberellic acid (GA, gibberellin A3, Sigma) was dissolved in Ethanol (10 mM stock solution) and applied to the MS-plates in concentrations from 0.01 µM to 10 µM. The germination rate of *fie* mutants on GA-plates was analyzed 10–14 days after stratification (DAS). Abscisic acid (ABA, Sigma) was dissolved in Methanol (stock concentration 10 mM) and used in final concentration of 1 µM. Wild type germination on ABA-plates was monitored over time.

Lipid staining

Plants were first partially dehydrated in three steps (20%, 40%, 60% isopropanole solution), then incubated for 1 hour with *Fat Red* solution (filtered 0.5% Sudan III in 60% isopropanole) and rehydrated again using the same dilution series in reversed direction. Subsequently samples were additionally washed twice with water and analyzed under a dissecting microscope.

RNA-extraction and qRT-PCR

RNA extraction was performed using Qiagen-RNAasy mini-kit, following the manufacturers instruction. RNA-concentration and

purity was tested using *nanodrop*-photometric quantification (Thermo Scientific). RNA-integrity was verified by running 1 µg of total RNA on 1.5% agarose TBE-gels to detect the 28S and 16S rRNA bands. 2 µg RNA was treated with DNaseI (MBI Fermentas) according to the manual to avoid contamination of genomic DNA and subsequently processed to obtain cDNA using polyT-primer and reverse transcriptase (Superscript III, Invitrogen) following the manufacturers instruction. After reverse transcription RNA was removed by RNaseH digest. For negative control, all steps were followed in the same manner, except for adding the reverse transcriptase. The resulting cDNA was used for Reverse Transcription(RT)-PCR or quantitative Real Time-PCR (qRT-PCR) using the Roche LightCycler 480 system. Oligonucleotides were designed using either Primer3Plus-design tool (<http://www.bioinformatics.nl/cgi-bin/primer3plus/primer3plus.cgi>) or QuantPrime (qPCR primer design tool: <http://www.quantprime.de/main>, [74] and used in final concentration of 0.25 µM each. Primers for qPCR have been tested for efficiency of >90% and are listed in Table S6. For qPCR at least two biological and three technical replicates were processed and expression was calculated relative to *ACT7* (*AT5G09810*). Several reference genes were tested in comparison between mutant and wild type samples to confirm equal loading (see Table S6).

Transcriptome assay

Microarray analysis was carried out at the Unité de Recherche en Génomique Végétale (Evry, France), using the CATMA arrays [75,76]. Two independent biological replicates were produced. For each biological repetition and each time point, RNA samples were obtained by pooling RNA from 100 wild-type and 100 *fie* seedlings at stage 7 DAS and 10 wild type and 50 *fie* plants at 20 DAS, respectively. 7 DAS stage plants were cultivated on plates, 20 DAS material was grown on plates for 10 days, then transferred to liquid media for another 10 days in day neutral conditions (12 h light, 21°C; 12 h dark, 17°C). Total RNA was extracted using Qiagen RNeasy plant mini kit according to the supplier's instructions. The hybridization to the slides, and the scanning were performed as described in Lurin et al. (2004) [77].

Normalization and statistical analysis were based on two dye swaps (i.e. four arrays, each containing 24,576 GSTs and 384 controls) as described in Gagnot et al. (2007) [78]. The raw P-values were adjusted by the Bonferroni method, which controls the Family Wise Error Rate, (with a type I error equal to 5%) in order to keep a strong control of the false positives in a multiple-comparison context [79]. We considered as being differentially expressed the genes with a Bonferroni P-value ≤0.05, as described in Gagnot et al (2007) [78].

Microarray data from this article were deposited at Gene Expression Omnibus (<http://www.ncbi.nlm.nih.gov/geo/>), accession no. GSE19851, direct link: <http://www.ncbi.nlm.nih.gov/geo/query/acc.cgi?token=djcpgeggksuirw&acc=GSE19851>) and at CATdb (<http://urgv.evry.inra.fr/CATdb/>; Project: RS08-09_FIE) according to the "Minimum Information About a Microarray Experiment" standards.

Western blot and peptide competition assay

Nuclear enriched protein extracts were prepared after thoroughly grinding in liquid nitrogen of around 1 g of plant material. All subsequent steps are carried out in the cold. The powder was dissolved in 10 ml of Lysis buffer (45 ml Low Salt Wash buffer [see below] + 0.5 ml TritonX-100 + 5 ml glycerol + 50 µl 100 mM PMSF + 20 µl β-mercaptoethanol freshly prepared on ice), vortexed and placed on a rotation wheel for 20 min at 4°C. The solution was filtered using 100 µm nylon mesh and centrifuged for

20 min at 4000 rpm at 4°C, following resuspension of the pellet in 2 ml lysis buffer. The solution was transferred to a new 2 ml tube and centrifuged for 20 min, 4000 rpm, 4°C. The resulting pellet was resuspended in 200 µl 1XSDS loading buffer. Low Salt Wash buffer: 20 ml 0.5 M HEPES pH 7.5 + 6 ml 5 M NaCl + 400 µl 500 mM EDTA + H₂O up to 200 ml. 15% SDS-gel page was performed according to standard protocols. After SDS page proteins were blotted on Hybond-P PVDF membrane (Amersham Biosciences) for 75 min, 140 mA in temperature controlled condition. All membrane manipulation experiments were carried out at room temperature (RT) when not stated otherwise. Membrane was blocked using incubation with 4XBlockAce (ABD Serotec) for 3 h. Throughout all experiments we used Anti-H3 1:20,000 (Millipore, reference nr: 06-755) as loading control, Anti-trimethyl-Histone H3 (Lys27) antibody (Millipore, reference-nr: 07-449) in final concentration between 1:10,000 and 1:50,000, dissolved in 5%BSA in 1xTBST (1x TBS with 0.1% TritonX-100) and Anti-trimethyl-Histone H3 (Lys4) antibody (Millipore, reference nr: 07-473) at 1:5,000–1:10,000. The primary antibody was incubated at 4°C over night. After washing 3 times 15 min with 1xTBST the secondary antibody (Anti-Rabbit antibody, GE-Healthcare, reference-nr: NA934-100UL) was applied at 1:50,000 in 5%BSA-1xTBST solution for 2 h. Washing was either performed stringently with 3x 30 min or less stringently 3x10 min. For detection the two-component reagent *Immobilion* Western Chemiluminiscent HRP substrate (Millipore) was used. For peptide competition, first the sub-saturating antibody concentration was determined. For anti-H3K27me3 this was at a concentration of 1:50,000. Then increasing concentrations from 0.1–10 µg of H3K27me3, H3K27me2 and H3K27me1 peptide (Millipore 12-565, 12-566, 12-567) were added to a 10 ml antibody-solution and incubated under slight agitation for 4 h at RT and an additional 1 h at 4°C before hybridizing on the membrane. Subsequent hybridization and detection were performed as described above.

ChIP-on-chip analysis

Chromatin immunoprecipitation (ChIP) experiments were done as described previously [74], in two biological replicates, using the following antibodies: H3K4me3, Millipore 07-473; H3K27me3, Millipore 07-449. DNA recovered after ChIP and directly from input chromatin was amplified using the Sigma GenomePlex Complete Whole Genome Amplification (WGA) Kit as directed, differentially labeled and hybridized in dye-swap experiments to a custom-made Roche-NimbleGen whole-genome tiling microarray. This microarray covers the entire forward strand of the Arabidopsis genome sequence (TAIR8) at 175 nt resolution with approx. 720K isothermal tiles (50–75 oligonucleotides). Following ANOVA normalization, raw data were analyzed using a linear regression mixture model (ChIPmix, [80]), which was adapted to handle multiple replicates simultaneously (script available on request). Lists of tiles reporting significant enrichment were converted in sets of chromatin domains by combining adjacent enriched tiles, allowing a maximal gap of 165 nucleotides. Only domains of at least 400 nucleotides were considered for further analysis. TAIR8 release was used for annotation of genes and transposable elements.

Several loci were additionally tested for H3K27me3 and H3K4me3 enrichment as compared to input. Input was diluted 1:100 prior to qPCR application. From the diluted input material and from the ChIP-material 1 µl was applied for each triple replicate reaction in the Roche Lightcycler 480 Real Time System using Roche SYBR green reagent according to the supplier's instruction (Roche). Primers used for this assay are given in Table S6.

ChIP on chip data from this article were deposited at Gene Expression Omnibus (<http://www.ncbi.nlm.nih.gov/geo/>), accession no. GSE24163, direct link: (GSE24163, <http://www.ncbi.nlm.nih.gov/geo/query/acc.cgi?acc=GSE24163>).

Immunocytology

10–14 DAS wild type and *fie* seedlings were fixed and processed as described previously [28], washed 3×5 min in 1× PBS before pre-incubation with BSA. Diluted rabbit polyclonal α - trimethyl H3K27 primary antibody (1:100, Millipore 07-449) was incubated for 1 h at 37°C, washed 3×5 min in 1× PBS and incubated with diluted Alexa Fluor 488 conjugated goat anti-rabbit polyclonal secondary antibody (1:200, Invitrogen (Molecular Probes) A-11008) for 1 h at 37°C, washed 3×5 min in 1× PBS and mounted in 1× PBS containing 1 µg/µl DAPI. Images were acquired using an Axioplan 2 Carl Zeiss Microscope with a cooled AxioCam HRC camera using a bandpass 515–565 nm emission filter (Carl Zeiss # 488010-9901-000) and a longpass 397 nm emission filter (Carl Zeiss # 488001-9901-000) for visualization of AF488 and DAPI, respectively. Fixed exposure settings for both fluorochromes were: AF488, 196 ms, 402 ms and 1002 ms (overexposure); DAPI, 50 ms, 100 ms and 305 ms (overexposure).

Data analysis

For all analyses comparing array expression and ChIP chip data a reference gene set of 24901 genes was defined that included those genes for which data from both type of experiments were available (Table S2). The Transcription factor classification was taken from the Arabidopsis transcription factor database (AtTFDB) hosted on the Arabidopsis Gene Regulatory Information Server (AGRIS, <http://arabidopsis.med.ohio-state.edu/AtTFDB>). Venn diagrams were generated using the VENN diagram generator designed by Tim Hulsen at <http://www.venndiagram.tk/> and <http://www.cmbi.ru.nl/cdd/biovenn/> (BioVenn [81]). The test for statistical significance of the overlap between two groups of genes was calculated by using software provided by Jim Lund accessible at http://elegans.uky.edu/MA/progs/overlap_stats.html. A representation factor (rf) is given and the probability (p) of finding an overlap of x genes is calculated using a hypergeometric probability formula. When p was below the calculation limits of the software (highly significant) we noted $p < 1.0e-99^*$. The representation factor is the number of overlapping genes divided by the expected number of overlapping genes drawn from two independent groups. A representation factor > 1 indicates more overlap than expected of two independent groups, a representation factor < 1 indicates less overlap than expected, and a representation factor of 1 indicates that the two groups by the number of genes expected for independent groups of genes. To determine which Gene Ontology (GO) categories are statistically overrepresented among the H3K27me3 targets that are up-regulated in *fie*, we used the BINGO 2.3 plugin for Cytoscape (<http://www.psb.ugent.be/cbd/papers/BiNGO/Home.html>). A custom annotation file was created using the build in annotation file for GO biological process and our reference set of 24901 genes. Other than that default parameters were used.

Supporting Information

Figure S1 Mutant alleles used in this study. (A) Graphic representation of the four different alleles that have been used in this study. GABI 534 and GABI 362 are both T-DNA insertion from the GABI-KAT collection with insertion sites in the 5th and 7th exon, respectively. EMS (G-A) has been previously described and shows a point mutation in the splice acceptor site at the 5' end

of exon 4 [83]. SALK 042 is a T-DNA insertion in exon 6 and is used as the reference allele throughout our analysis. Arrows indicate RT-PCR primer binding sites; arrowheads show the position of the qRT-PCR primer-set. (B) RT-PCR analysis of *FIE* expression in two replicates of wild type and the *fie*-SALK 042 mutant, respectively. The small subunit 5a of ribulose1,5 biphosphate carboxylase (*RBC*) is used as a reference control gene and shows comparable levels in expression between wild type and *fie* whereas *FIE* is not detected in the mutant. Negative controls without reverse transcriptase (RT) show no signal with both *RBC* and *FIE* primer mix. Genomic DNA (gDNA) shows a remarkably longer fragment in wild type but is undetectable in the *fie*-T-DNA mutant most likely due to the large increase of the amplicon. (C) Shows the results of the qRT-PCR analysis of *fie*-SALK 042 relative to the ACTIN 7 gene (ACT7). Expression is barely detectable and remaining signal is 10,000 times or more reduced in the mutant (two replicates are shown for both, wild type and mutant).

(TIF)

Figure S2 Flow cytometrical analyses. Flow cytometry experiments with wild type and *fie* plants at 20 DAS reveal lower ploidy level in the mutant (A,B,D). Callus-like *fie* mutants at 3 months contain mainly 2C and 4C nuclei (C) and are strongly reduced in endoreplication (C,D).

(TIF)

Figure S3 Loss of H3K27me3 signal in *fie* mutants. Immunohistochemical visualisation of H3K27me3 in interphase nuclei of wild type (WT) (A–C) and *fie* mutant seedlings (D–F). All samples were treated equally and images were acquired with fixed exposure settings. The first columns show DAPI staining of interphase nuclei (A1–F1). No obvious difference was found in nuclear morphology or chromocenter distribution between wild type and *fie*. The AlexaFluor488 conjugated secondary antibody was used to visualize H3K27 trimethylation. Column two (antibody) shows normal exposure (196 ms) and column three (antibody-OE) overexposure (1002 ms). (A–C) In wild type the H3K27me3 signal is found in a widely dispersed pattern along the entire chromatin and does not paint compacted heterochromatic regions (A1–C1, A2–C2). (D–F) No antibody signal could be obtained in *fie* nuclei using normal exposure settings (D2–F2). Overexposure revealed a faint signal in some *fie* mutant nuclei (D3, F3).

(TIF)

Figure S4 ChIP-on-chip experiments using an H3K27me3 antibody reveals overlapping gene classes in wild type and *fie* mutants. VENN Diagram representing the number of genes detected by an H3K27me3 antibody in ChIP-on-chip experiments. The red circle represents data generated from 10–14 day old seedlings by Zhang. *et al* (2007). Genes identified in this study from 20 DAS wild type and *fie* mutants are shown in green and yellow, respectively. Several lines of evidence indicate, that the genes detected in *fie* are not H3K27me3 positive, but were labeled in *fie* due to cross-reactivity of the antibody and the absence of the proper antigen.

(TIF)

Figure S5 Atypical H3K27me3 signal in *fie*. Examples of H3K27me3 ChIP-chip signal in *fie*. (A–C) First upper panels show H3K27me3 signal of wild type and *fie*, respectively. Lower two panels represent genes (blue = exons, grey = introns) and transposable elements (brown, orange = coding sequences). (A) Shows signal of *Atlg02190*, which is restricted to the very N-terminal part whereas in wild type a typical signal distribution

covers the whole coding region, (see the two genes downstream of *Atlg02190* as an example). (B) Often the signal in *fie* appears in and close to heterochromatic region, where it is typically absent in wild type. (C) Example of a gain with spotty appearance of H3K27me3 signal in *fie* at *Atlg96360*.

(TIF)

Figure S6 ChIP-qPCR validation. (A) H3K27me3 ChIP qPCR for 10 loci and (B) H3K4me3 ChIP qPCR for 6 loci from wild type (wild type) and *fie* mutant material. The result is given in % of ChIP-input. (A) For all genes H3K27me3 levels in *fie* drop to the signal intensity of the negative control, i.e a gene that showed no H3K27me3 mark in wild type (*At5g13440*). When performing ChIP qPCR for specific heterochromatic loci (AtenSAT, VANDAL4, ATGP1), which showed significant enrichment in our ChIP-array (see E, F), we find a slight increase in signal strength in *fie*, but the signal strength is clearly below H3K27me3-positive genic loci. For most genes H3K4me3 is not changed between wild type and *fie*. (B) Shows H3K4me3 ChIP qRT results in accordance with our ChIP array and (C) shows a Western analysis for H3K4me3. Histone H3 is used as a loading control in (C). Examples for ChIP-chip results are shown in (D–F). The first two panels show wild type and *fie* signal for H3K27me3, respectively, the third panel shows TAIR8-representation of genes (blue = exon, grey = intron) and transposable element loci (brown = transposable elements, orange = transposable element coding region). In (D) the lower two panels show H3K4me3 signal in wild type and *fie*, respectively. Upon loss of H3K27me3 there is gain in H3K4me3 in *fie* at the AG locus (D). The transposable elements AT4TE27915 (ATGP1) (E) and AT4TE08945 (AtenSAT) (F) show significant gain in contrast to ChIP-qPCR results (A).

(TIF)

Figure S7 Only a fraction of H3K27me3 targets are deregulated in *fie* mutants. VENN Diagram representing genes significantly up-regulated (A) and down-regulated (B) in *fie* after 7 and 20 DAS in relation to the set of H3K27me3 marked genes in wild type. The gene numbers are given with respect to the reference gene set (24901 genes). The mutual overlap of the gene sets in A (up-regulation) is larger than expected for the two independent groups in all three cases (7 DAS and 20 DAS: representation factor (rf) = 7.1, $p < 1.0e-99$ *; 7 DAS and H3K27me3: rf = 1.6, $p < 1.8e-21$; 20 DAS and H3K27me3: rf = 1.1, $p < 0.009$). The mutual overlap of the gene sets in B (down-regulation) is larger than expected of two independent groups for 7 DAS and 20 DAS, but smaller or as expected of two independent groups for the other two cases (7 DAS and 20 DAS: rf = 7.5, $p < 1.0e-99$ *; 7 DAS and H3K27me3: rf = 0.6, $p < 1.3e-13$; 20 DAS and H3K27me3: rf = 0.9, $p < 0.122$). P-values marked by an asterisk (*) were below the calculation limits of the software (highly significant).

(TIF)

Figure S8 Overrepresented gene ontology categories in the set of H3K27me3 targets that are up-regulated in *fie*. BiNGO (the Biological Network Gene Ontology tool) analysis representing over-represented categories of the ontology *Biological Process* among the genes that are marked by H3K27me3 in the wild type (20 DAS) and significantly up-regulated in 20 DAS *fie* mutant seedlings. The size of the nodes is proportional to the number of genes in the test set which are annotated to that node. Colored nodes are significantly over-represented, with a color scale ranging from yellow (p-value = 0.05) to dark orange (p-value = 5.00^E-7). Statistical testing was as described by Maere *et al.* (2005) [31].

(TIF)

Figure S9 PRC2 targets involved in flower development. Genes marked by H3K27me3 in the wild type and that are up-regulated in *fie* mutants are colored in red (significant up-regulation seen on CATMA array) or encircled in red (up-regulation only seen in qRT PCR). Genes that are not up-regulated in *fie* but are trimethylated at K27 in the wild type are labeled in orange. Arrows indicate activation, bars indicate inhibition. Dotted lines (C) or overlapping ovals (A–C) mark protein-protein interactions. For a detailed description of the pathways depicted here see Liu et al. (2010) and Irish (2010) [84,85]. (A) Establishment of a floral meristem, modified after Liu et al. (2010) [85]. (B) Control of floral meristem determinacy, modified after Irish (2010) [84]. (C) Floral organ identity specification, modified after Irish (2010) [84]. (TIF)

Figure S10 Expression analysis of LEA proteins deregulated in *fie* mutants. Heat map display of a Genevestigator analysis (anatomy view) of the LEA genes that were differentially expressed in *fie* mutants (www.genevestigator.com). The numbers of arrays analyzed for the respective plant structures are given next to each row. Wild type, non-stimulated high quality expression arrays were selected. Only LEAs for which a unique probe in the Genevestigator analysis could be found are displayed. The LEA proteins were grouped regarding H3K27 trimethylation status in wild type and deregulation in *fie*. Block 1 shows all genes that carry a H3K27me3 mark in the wild type which are up-regulated in *fie*, Block 2 represents genes up-regulated in *fie*, but for which no H3K27me3 mark could be detected in wild type at 20 DAS and block 3 represents genes that were significantly down-regulated in *fie*, one of which carried a H3K27me3 mark in wild type (*). Expression values displayed in the heat map are scaled to the expression potential of each gene. The expression potential of each gene is shown as a small green histogram below the heat map. The darkest blue color represents the maximum level of expression for a given gene across all measurements available in the database. (TIF)

Figure S11 Differences in H3K27 Trimethylation and up-regulation in *fie* among the different transcription factor families. On the X-axis the different transcription factor (TF) families are listed, the Y-axis displays the amount of TFs in absolute numbers (A) or in percentage with respect to the reference set (B). Grey bars represent the TFs found in the reference set, green bars the TFs that are labeled by H3K27me3 and red bars the TFs that are H3K27me3 marked and up-regulated in *fie* at 7 and/or 20 DAS. The TF families are ordered by decreasing percentage of H3K27 trimethylated members (TIF)

Table S1 H3K27me3 and H3K4me3 marked genes in wild type and *fie* mutant seedlings. Lists of genes significantly enriched for marks recognized by the H3K27me3 in wild type or the H3K4me3 antibody in wild type or *fie* mutants at 20 DAS. The raw data can be downloaded from GEO accession viewer (GSE24163, <http://www.ncbi.nlm.nih.gov/geo/query/acc.cgi?acc=GSE24163>). (XLS)

Table S2 Disparity of H3K27me3 signal in wild type and *fie* mutants. Wild type and *fie* show differences in signal strength and in the properties of genes that were recognized by the H3K27me3

antibody in ChIP-on-chip experiments, suggesting that the signal in *fie* is not a true H3K27me3 signal. (DOC)

Table S3 List of the reference set of genes with expression data and ChIP chip data generated in this study. Expression array raw data were deposited at Gene Expression Omnibus (GEO-Nr: GSE19851): <http://www.ncbi.nlm.nih.gov/geo/query/acc.cgi?token=djcjpeggkgsuirw&acc=GSE19851> and at CATdb (<http://urgv.evry.inra.fr/CATdb/> project-number: RS08-09_FIE) The raw data for the ChIP chip experiments is deposited at GEO (in preparation). (XLS)

Table S4 Quantification of RNA expression level by qRT-PCR. Genes of different functional categories (flowering, meristem, root, seed, or reference gene) were tested for expression by qRT-PCR in wild type and *fie* mutants. Material from 2 different time points was tested (7 and 20 DAS). The values in column 4–7 are given relative to *ACTIN7* (*ACT7*). Standard deviations (STDV) are given in columns 8–10. The columns 11 and 12 of the table shows the ratios between *fie*/wild type for 7 and 20 DAS as well as *fie* 7DAS and *fie* 20DAS to compare the expression level differences between mutant and wild type, as well as between the late and the early time point in case of the *fie* mutant. The last four columns show the results from the CATMA array in comparison. (XLS)

Table S5 Expression and H3K27 and H3K4 Trimethylation analysis of different gene families. Detailed analysis of AGL transcription factors, WOX transcription factors, LEAs and oleosins with respect to expression and ChIP-on-chip data generated in this study. Gene families were taken from deFolter et al. for AGL (2005), Graaff et al. for WOX (2009), Hundertmark et al., Bies-Ethève et al. for LEAs (2008) and Kim et al. for Oleosins (2002) [34–37,82]. (XLS)

Table S6 Oligonucleotide sequences used in this study. List of all primer sequences for qRT-PCR, ChIP-qPCR and genotyping. For each category, oligonucleotides are listed according to their AGI (TAIR9), gene names are given in the second column. Amplicon size is indicated for qPCR-primers. FWD = forward primer sequence. REV = reverse primer sequence. For genotyping FWD and REV primers will amplify wild type sequence, to amplify T-DNA-specific sequence, the respective T-DNA LB-primer is used in combination with FWD primer. (DOC)

Acknowledgments

We would like to thank Hirofumi Harashima for advice in Western blot experiments. Gaëtan Pochon is kindly acknowledged for his assistance in plant work.

Author Contributions

Conceived and designed the experiments: DB FR MH MKN JG JPR PEG VC AS. Performed the experiments: DB FR EDA DG MKN. Analyzed the data: DB FR MH EDA DG MKN JG JPR PEG VC AS. Wrote the paper: DB FR MH PEG VC AS.

References

- Finkelstein R, Reeves W, Ariizumi T, Steber C (2008) Molecular aspects of seed dormancy. *Annu Rev Plant Biol* 59: 387–415.
- He Y (2009) Control of the transition to flowering by chromatin modifications. *Molecular Plant* 2: 554–564.

3. Farrona S, Coupland G, Turck F (2008) The impact of chromatin regulation on the floral transition. *Seminars in Cell & Developmental Biology* 19: 560–573.
4. Kim DH, Doyle MR, Sung S, Amasino RM (2009) Vernalization: winter and the timing of flowering in plants. *Annu Rev Cell Dev Biol* 25: 277–299.
5. Kinoshita T, Harada JJ, Goldberg RB (2001) Polycomb repression of flowering during early plant development. *Proceedings of the National Academy of Sciences*.
6. Chanvivattana Y, Bishopp A, Schubert D, Stock C, Moon YH, et al. (2004) Interaction of Polycomb-group proteins controlling flowering in Arabidopsis. *Development* 131: 5263–5276.
7. Schuettengruber B, Chourrout D, Vervoort M, Leblanc B, Cavalli G (2007) Genome regulation by polycomb and trithorax proteins. *Cell* 128: 735–745.
8. Schwartz YB, Pirrotta V (2008) Polycomb complexes and epigenetic states. *Current Opinion in Cell Biology* 20: 266–273.
9. Papp B, Müller J (2006) Histone trimethylation and the maintenance of transcriptional ON and OFF states by trxG and PcG proteins. *Genes & Development* 20: 2041–2054.
10. Bantignies F, Cavalli G (2006) Cellular memory and dynamic regulation of polycomb group proteins. *Current Opinion in Cell Biology* 18: 275–283.
11. Kohler C, Villar CB (2008) Programming of gene expression by Polycomb group proteins. *Trends Cell Biol* 18: 236–243.
12. Pien S, Grossniklaus U (2007) Polycomb group and trithorax group proteins in Arabidopsis. *BBA-Genes Structure and Expression* 1769: 375–382.
13. Simon J, Chiang A, Bender W (1992) Ten different Polycomb group genes are required for spatial control of the *abdA* and *AbdB* homeotic products. *Development* 114: 493–505.
14. Struhl G, Akam M (1985) Altered distributions of Ultrabithorax transcripts in extra sex combs mutant embryos of *Drosophila*. *EMBO J* 4: 3259–3264.
15. Faust C, Schumacher A, Holdener B, Magnuson T (1995) The *ced* mutation disrupts anterior mesoderm production in mice. *Development* 121: 273–285.
16. Huh JH, Bauer MJ, Hsieh T, Fischer R (2007) Endosperm gene imprinting and seed development. *Current opinion in genetics & development* 17: 480–485.
17. Berger F, Chaudhury A (2009) Parental memories shape seeds. *Trends in Plant Science* 14: 550–556.
18. Kinoshita T, Ikeda Y, Ishikawa R (2008) Genomic imprinting: A balance between antagonistic roles of parental chromosomes. *Seminars in Cell and Developmental Biology* 19: 574–579.
19. Baroux C, Pien S, Grossniklaus U (2007) Chromatin modification and remodeling during early seed development. *Current opinion in genetics & development* 17: 473–479.
20. Katz A, Oliva M, Mosquana A, Hakim O, Ohad N (2004) FIE and CURLY LEAF polycomb proteins interact in the regulation of homeobox gene expression during sporophyte development. *Plant J* 37: 707–719.
21. Aw SJ, Hamamura Y, Chen Z, Schnittger A, Berger F (2010) Sperm entry is sufficient to trigger division of the central cell but the paternal genome is required for endosperm development in Arabidopsis. *Development*.
22. Nowack MK, Grini PE, Jakoby MJ, Lafos M, Koncz C, et al. (2006) A positive signal from the fertilization of the egg cell sets off endosperm proliferation in angiosperm embryogenesis. *Nat Genet* 38: 63–67.
23. Iwakawa H, Shinmyo A, Sekine M (2006) Arabidopsis CDKA1;1, a *cdc2* homologue, controls proliferation of generative cells in male gametogenesis. *Plant J* 45: 819–831.
24. Nowack MK, Shirzadi R, Dissmeyer N, Dolf A, Endl E, et al. (2007) Bypassing genomic imprinting allows seed development. *Nature* 447: 312–315.
25. Kurzhals RL, Tie F, Stratton CA, Harte PJ (2008) *Drosophila* ESC-like can substitute for ESC and becomes required for Polycomb silencing if ESC is absent. *Developmental Biology* 313: 293–306.
26. Bramsiepe J, Schnittger A (submitted) Endoreplication and development. *Plant Signaling & Behavior*.
27. Lindroth AM, Shultis D, Jasencakova Z, Fuchs J, Johnson L, et al. (2004) Dual histone H3 methylation marks at lysines 9 and 27 required for interaction with CHROMOMETHYLASE3. *EMBO J* 23: 4286–4296.
28. Naumann K, Fischer A, Hofmann I, Krauss V, Phalke S, et al. (2005) Pivotal role of AtSUVH2 in heterochromatic histone methylation and gene silencing in Arabidopsis. *EMBO J* 24: 1418–1429.
29. Zhang X, Clarenz O, Cokus S, Bernatavichute Y, Pellegrini M, et al. (2007) Whole-genome analysis of histone H3 lysine 27 trimethylation in Arabidopsis. *PLoS Biol* 5: e129. doi:10.1371/journal.pbio.0050129.
30. Jacob Y, Stroud H, Leblanc C, Feng S, Zhou L, et al. (2010) Regulation of heterochromatic DNA replication by histone H3 lysine 27 methyltransferases. *Nature*;2010 Jul 14.
31. Maere S, Heymans K, Kuiper M (2005) BiNGO: a Cytoscape plugin to assess overrepresentation of gene ontology categories in biological networks. *Bioinformatics* 21: 3448–3449.
32. Yoshida N, Yanai Y, Chen L, Kato Y, Hiratsuka J, et al. (2001) EMBRYONIC FLOWER2, a novel polycomb group protein homolog, mediates shoot development and flowering in Arabidopsis. *The Plant Cell* 13: 2471–2481.
33. Turck F, Roudier F, Farrona S, Martin-Magniette ML, et al. (2007) Arabidopsis TFL2/LHP1 specifically associates with genes marked by trimethylation of histone H3 lysine 27. *PLoS Genet* 3: e86. doi:10.1371/journal.pgen.0030086.
34. de Folter S, Immink RG, Kieffer M, Parenicová L, Henz SR, et al. (2005) Comprehensive interaction map of the Arabidopsis MADS Box transcription factors. *The Plant Cell* 17: 1424–1433.
35. Kim HU, Hsieh K, Ratnayake C, Huang AH (2002) A novel group of oleosins is present inside the pollen of Arabidopsis. *J Biol Chem* 277: 22677–22684.
36. Hundertmark M, Hinch DK (2008) LEA (late embryogenesis abundant) proteins and their encoding genes in Arabidopsis thaliana. *BMC Genomics* 9: 118.
37. Bies-Ethève N, Gaubier-Comella P, Debures A, Lasserre E, Jobet E, et al. (2008) Inventory, evolution and expression profiling diversity of the LEA (late embryogenesis abundant) protein gene family in Arabidopsis thaliana. *Plant Mol Biol* 67: 107–124.
38. Alvarez-Venegas R, Pien S, Sadler M, Witmer X, Grossniklaus U, et al. (2003) ATX-1, an Arabidopsis homolog of trithorax, activates flower homeotic genes. *Curr Biol* 13: 627–637.
39. Tamada Y, Yun JY, Woo SC, Amasino RM (2009) ARABIDOPSIS TRITHORAX-RELATED7 is required for methylation of lysine 4 of histone H3 and for transcriptional activation of FLOWERING LOCUS C. *The Plant Cell* 21: 3257–3269.
40. Berr A, Xu L, Gao J, Cognat V, Steinmetz A, et al. (2009) SET DOMAIN GROUP25 encodes a histone methyltransferase and is involved in FLOWERING LOCUS C activation and repression of flowering. *PLANT PHYSIOLOGY* 151: 1476–1485.
41. Aichinger E, Villar CB, Farrona S, Reyes JC, Hennig L, et al. (2009) CHD3 proteins and polycomb group proteins antagonistically determine cell identity in Arabidopsis. *PLoS Genet* 5: e1000605. doi:10.1371/journal.pgen.1000605.
42. Carles CC, Fletcher J (2009) The SAND domain protein ULTRAPETAL1 acts as a trithorax group factor to regulate cell fate in plants. *Genes & Development* 23: 2723–2728.
43. Zhang X, Bernatavichute YV, Cokus S, Pellegrini M, Jacobsen SE (2009) Genome-wide analysis of mono-, di- and trimethylation of histone H3 lysine 4 in Arabidopsis thaliana. *Genome Biol* 10: R62.
44. Saleh A, Al-Abdallat A, Ndamukong I, Alvarez-Venegas R, Avramova Z (2007) The Arabidopsis homologs of trithorax (ATX1) and enhancer of zeste (CLF) establish 'bivalent chromatin marks' at the silent AGAMOUS locus. *Nucleic Acids Research* 35: 6290–6296.
45. Pien S, Fleury D, Mylne JS, Crevillen P, Inzé D, et al. (2008) ARABIDOPSIS TRITHORAX1 dynamically regulates FLOWERING LOCUS C activation via histone 3 lysine 4 trimethylation. *The Plant Cell* 20: 580–588.
46. Akkers RC, van Heeringen SJ, Jacobi UG, Janssen-Megens EM, François KJ, et al. (2009) A hierarchy of H3K4me3 and H3K27me3 acquisition in spatial gene regulation in *Xenopus* embryos. *Developmental Cell* 17: 425–434.
47. Ku M, Koche RP, Rheinbay E, Mendenhall EM, Endoh M, et al. (2008) Genome-wide analysis of PRC1 and PRC2 occupancy identifies two classes of bivalent domains. *PLoS Genet* 4: e1000242. doi:10.1371/journal.pgen.1000242.
48. Mikkelsen TS, Ku M, Jaffe DB, Issac B, Lieberman E, et al. (2007) Genome-wide maps of chromatin state in pluripotent and lineage-committed cells. *Nature* 448: 553–560.
49. Pan G, Tian S, Nie J, Yang C, Ruotti V, et al. (2007) Whole-genome analysis of histone H3 lysine 4 and lysine 27 methylation in human embryonic stem cells. *Cell Stem Cell* 1: 299–312.
50. Zhao XD, Han X, Chew JL, Liu J, Chiu KP, et al. (2007) Whole-genome mapping of histone H3 Lys4 and 27 trimethylations reveals distinct genomic compartments in human embryonic stem cells. *Cell Stem Cell* 1: 286–298.
51. Gan Q, Schones DE, Ho Eun S, Wei K, Cui K, et al. (2010) Monovalent and unpoised status of most genes in undifferentiated cell-enriched *Drosophila* testis. *Genome Biol* 11: R42.
52. Jeong JH, Song HR, Ko JH, Jeong YM, Kwon YE, Seol JH, et al. (2009) Repression of FLOWERING LOCUS T chromatin by functionally redundant histone H3 lysine 4 demethylases in Arabidopsis. *PLoS ONE* 4: e8033. doi:10.1371/journal.pone.0008033.
53. Schlereth A, Möller B, Liu W, Kientz M, Flippe J, et al. (2010) MONOPTEROS controls embryonic root initiation by regulating a mobile transcription factor. *Nature* 464: 913–916.
54. Lau S, Ehrismann JS, Schlereth A, Takada S, Mayer U, et al. (2010) Cell-cell communication in Arabidopsis early embryogenesis. *Eur J Cell Biol* 89: 225–230.
55. Amasino R (2010) Seasonal and developmental timing of flowering. *Plant J* 61: 1001–1013.
56. Dennis ES, Peacock WJ (2007) Epigenetic regulation of flowering. *Current Opinion in Plant Biology* 10: 520–527.
57. Henderson IR, Dean C (2004) Control of Arabidopsis flowering: the chill before the bloom. *Development* 131: 3829–3838.
58. Zhang H, Ogas J (2009) An Epigenetic Perspective on Developmental Regulation of Seed Genes. *Molecular Plant* 2: 610–627.
59. North H, Baud S, Debeaujon I, Dubos C, Dubreucq B, et al. (2010) Arabidopsis seed secrets unravelled after a decade of genetic and omics-driven research. *Plant J* 61: 971–981.
60. Junker A, Hartmann A, Schreiber F, Baumlein H (2010) An engineer's view on regulation of seed development. *Trends in plant science*.
61. Holdsworth MJ, Bentsink L, Soppe WJ (2008) Molecular networks regulating Arabidopsis seed maturation, after-ripening, dormancy and germination. *New Phytol* 179: 33–54.
62. Bentsink L, Jowett J, Hanhart CJ, Koornneef M (2006) Cloning of DOG1, a quantitative trait locus controlling seed dormancy in Arabidopsis. *Proc Natl Acad Sci USA* 103: 17042–17047.

63. Liu Y, Koornneef M, Soppe WJ (2007) The absence of histone H2B monoubiquitination in the *Arabidopsis* *hub1* (*rdo4*) mutant reveals a role for chromatin remodeling in seed dormancy. *The Plant Cell* 19: 433–444.
64. Alonso-Blanco C, Bentsink L, Hanhart CJ, Blankestijn-de Vries H, Koornneef M (2003) Analysis of natural allelic variation at seed dormancy loci of *Arabidopsis thaliana*. *Genetics* 164: 711–729.
65. Finch-Savage WE, Leubner-Metzger G (2006) Seed dormancy and the control of germination. *New Phytol* 171: 501–523.
66. Chiang GC, Barua D, Kramer EM, Amasino RM, Donohue K (2009) Major flowering time gene, flowering locus C, regulates seed germination in *Arabidopsis thaliana*. *Proc Natl Acad Sci USA* 106: 11661–11666.
67. Mosquna A, Katz A, Decker EL, Rensing SA, Reski R, et al. (2009) Regulation of stem cell maintenance by the Polycomb protein FIE has been conserved during land plant evolution. *Development* 136: 2433–2444.
68. Okano Y, Aono N, Hiwatashi Y, Murata T, Nishiyama T, et al. (2009) A polycomb repressive complex 2 gene regulates apogamy and gives evolutionary insights into early land plant evolution. *Proc Natl Acad Sci USA* 106: 16321–16326.
69. Ohad N, Margossian L, Hsu YC, Williams C, Repetti P, et al. (1996) A mutation that allows endosperm development without fertilization. *Proc Natl Acad Sci U S A* 93: 5319–5324.
70. Ingouff M, Haseloff J, Berger F (2005) Polycomb group genes control developmental timing of endosperm. *Plant J* 42: 663–674.
71. Luo M, Bilodeau P, Dennis ES, Peacock WJ, Chaudhury A (2000) Expression and parent-of-origin effects for FIS2, MEA, and FIE in the endosperm and embryo of developing *Arabidopsis* seeds. *Proc Natl Acad Sci U S A* 97: 10637–10642.
72. Doyle MR, Amasino RM (2009) A single amino acid change in the enhancer of zeste ortholog CURLY LEAF results in vernalization-independent, rapid flowering in *Arabidopsis*. *PLANT PHYSIOLOGY* 151: 1688–1697.
73. Wang D, Tyson MD, Jackson SS, Yadegari R (2006) Partially redundant functions of two SET-domain polycomb-group proteins in controlling initiation of seed development in *Arabidopsis*. *Proc Natl Acad Sci USA* 103: 13244–13249.
74. Arvidsson S, Kwasniewski M, Riaño-Pachón DM, Mueller-Roeber B (2008) QuantPrime—a flexible tool for reliable high-throughput primer design for quantitative PCR. *BMC Bioinformatics* 9: 465.
75. Crowe ML, Serizet C, Thareau V, Aubourg S, Rouzé P, et al. (2003) CATMA: a complete *Arabidopsis* GST database. *Nucleic Acids Research* 31: 156–158.
76. Hilson P, Allemeersch J, Altmann T, Aubourg S, Avon A, et al. (2004) Versatile gene-specific sequence tags for *Arabidopsis* functional genomics: transcript profiling and reverse genetics applications. *Genome Research* 14: 2176–2189.
77. Lurin C, Andrés C, Aubourg S, Bellaoui M, Bitton F, et al. (2004) Genome-wide analysis of *Arabidopsis* pentatricopeptide repeat proteins reveals their essential role in organelle biogenesis. *The Plant Cell* 16: 2089–2103.
78. Gagnot S, Tamby JP, Martin-Magniette ML, Bitton F, Taconnat L, et al. (2008) CATdb: a public access to *Arabidopsis* transcriptome data from the URGV-CATMA platform. *Nucleic Acids Research* 36: D986–90.
79. Ge X, Tsutsumi S, Aburatani H, Iwata S (2003) Reducing false positives in molecular pattern recognition. *Genome informatics International Conference on Genome Informatics* 14: 34–43.
80. Martin-Magniette ML, Mary-Huard T, Bérard C, Robin S (2008) ChIPmix: mixture model of regressions for two-color ChIP-chip analysis. *Bioinformatics* 24: i181–6.
81. Hulsen T, de Vlieg J, Alkema W (2008) BioVenn - a web application for the comparison and visualization of biological lists using area-proportional Venn diagrams. *BMC Genomics* 9: 488.
82. van der Graaff E, Laux T, Rensing SA (2009) The WUS homeobox-containing (WOX) protein family. *Genome Biol* 10: 248.
83. Ohad N, Yadegari R, Margossian L, Hannon M, Michaeli D, et al. (1999) Mutations in FIE, a WD polycomb group gene, allow endosperm development without fertilization. *The Plant Cell* 11: 407–416.
84. Irish VF (2010) The flowering of *Arabidopsis* flower development. *Plant J* 61: 1014–1028.
85. Liu C, Thong Z, Yu H (2009) Coming into bloom: the specification of floral meristems. *Development* 136: 3379–3391.